

Materials Horizons

Accepted Manuscript

This article can be cited before page numbers have been issued, to do this please use: J. E. Kim, K. Soh, S. Hwang, D. Y. Yang and J. H. Yoon, *Mater. Horiz.*, 2025, DOI: 10.1039/D5MH00038F.



This is an Accepted Manuscript, which has been through the Royal Society of Chemistry peer review process and has been accepted for publication.

Accepted Manuscripts are published online shortly after acceptance, before technical editing, formatting and proof reading. Using this free service, authors can make their results available to the community, in citable form, before we publish the edited article. We will replace this Accepted Manuscript with the edited and formatted Advance Article as soon as it is available.

You can find more information about Accepted Manuscripts in the [Information for Authors](#).

Please note that technical editing may introduce minor changes to the text and/or graphics, which may alter content. The journal's standard [Terms & Conditions](#) and the [Ethical guidelines](#) still apply. In no event shall the Royal Society of Chemistry be held responsible for any errors or omissions in this Accepted Manuscript or any consequences arising from the use of any information it contains.

Wider impact

The implementation of artificial sensory systems is essential for converting vast amounts of environmental information into input signals required for neuromorphic computing. When realized using memristors, such systems effectively compress signals during the conversion process while retaining adaptive, nociceptive, and spatiotemporal information critical for learning and inference. Furthermore, their compatibility with a wide range of sensors ensures excellent expandability, while the dynamic resistive switching properties of memristors enable diverse signal conversion strategies. Memristor-based artificial sensory systems not only emulate human sensory processing but also offer significant advantages in terms of energy efficiency and miniaturization, making them highly suitable for edge computing and wearable technologies. Their ability to perform parallel signal processing can also enhance real-time decision-making in complex environments. Gaining insights into memristor-based artificial sensory systems, which process patterned sensory data akin to human perception, can drive future advancements in neuromorphic computing, industrial automation, and robotics.



Journal Name

ARTICLE

View Article Online
DOI: 10.1039/D5MH00038F

Data availability statement

No primary research results, software or code have been included and no new data were generated or analysed as part of this review.

Open Access Article. Published on 07 mars 2025. Downloaded on 2025-03-09 22:28:08.
This article is licensed under a Creative Commons Attribution-NonCommercial 3.0 Unported Licence.



Materials Horizons Accepted Manuscript

REVIEW

Memristive Neuromorphic Interfaces: Integrating Sensory Modalities with Artificial Neural Networks

Ji Eun Kim^{a,b,t}, Keunho Soh^{c,t}, Suin Hwang^c, Do Young Yang^c, and Jung Ho Yoon^{c*}

Received 00th January 20xx,

Accepted 00th January 20xx

DOI: 10.1039/x0xx00000x

The advent of the Internet of Things (IoT) has led to exponential growth in data generated from sensors, requiring efficient methods to process complex and unstructured external information. Unlike conventional von Neumann sensory systems with separate data collection and processing units, biological sensory systems integrate sensing, memory, and computing to process environmental information in real time with high efficiency. Memristive neuromorphic sensory systems using memristors as their basic components have emerged as promising alternatives to CMOS-based systems. Memristors can closely replicate the key characteristics of biological receptors, neurons, and synapses by integrating the threshold and adaptation properties of receptors, the action potential firing in neurons, and the synaptic plasticity of synapses. Furthermore, through careful engineering of their switching dynamics, the electrical properties of memristors can be tailored to emulate specific functions, while benefiting from high operational speed, low power consumption, and exceptional scalability. Consequently, their integration with high-performance sensors offers a promising pathway toward realizing fully integrated artificial sensory systems that can efficiently process and respond to diverse environmental stimuli in real time. In this review, we first introduce the fundamental principles of memristive neuromorphic technologies for artificial sensory systems, explaining how each component is structured and what functions they perform. We then discuss how these principles can be applied to replicate the four traditional senses, highlighting the underlying mechanisms and recent advances in mimicking biological sensory functions. Finally, we address the remaining challenges and provide prospects for the continued development of memristor-based artificial sensory systems.

1. Introduction

The growing demand for automation in supply chains, manufacturing, robotics, and unmanned vehicles has driven the development of artificial intelligence (AI) technologies. These technologies have the potential to significantly improve efficiency and autonomy across various industries using sensory systems comprising sensors and computational networks to sense the surroundings and acquire information from the environment in real time.^{1, 2} For instance, conventional complementary metal-oxide semiconductor (CMOS)-based systems have demonstrated intelligent recognition and control applications, such as image classification, natural language processing, and decision-making tasks.^{3–10} However, because the von Neumann architecture physically separates memory and processing units, conventional systems require massive amounts of data transfer between them. This results in high power consumption and causes significant latency, commonly referred to as the von Neumann bottleneck, which fundamentally degrades the performance of AI applications.

Unlike conventional systems, biological sensory systems detect, interpret, and store external information in a data-parallel and integrated manner.¹⁵ This is enabled by receptors that generate electrical signals only when stimuli exceed a threshold, selectively adapting to harmless, repetitive inputs. These signals are transmitted as action potentials (spikes) through neurons to specific brain regions, where they are processed in an event-driven, adaptive, and parallel manner, enabling learning and inference.^{16, 17} Inspired by the energy-efficient and fault-tolerant nature of biological systems, neuromorphic computing has been developed to overcome the technical limitations of conventional CMOS-based systems.^{18–21} It supports the integration, processing, and storage of sensory information, playing a crucial role in advanced functions, such as decision-making, cognition, learning, and memory. Moreover, neuromorphic computing can execute multiple tasks simultaneously in highly parallel settings with a low power consumption of 1–100 fJ per synaptic event.²² The exceptional capabilities of memristors enable their integration with neuromorphic learning algorithms to facilitate advanced functions. Large-scale integration and hardware implementation using CMOS-compatible processes are essential to leverage these capabilities, with extensive research currently underway. The technology has now advanced beyond hybrid 1T1R structures, reaching a stage where fully memristor-based hardware implementations are feasible. This progress has demonstrated the practical applicability of memristors across various AI applications, validating their potential for widespread deployment.^{23–27}

Therefore, it is crucial to implement artificial sensory systems capable of mimicking the roles of biological receptors, neurons, and

^a Electronic Materials Research Center, Korea Institute of Science and Technology (KIST), Seoul 02791 Republic of Korea Address here.

^b Department of Materials Science and Engineering, Korea University, Seoul 02841, Republic of Korea

^c School of Advanced Materials and Engineering, Sungkyunkwan University (SKKU), Suwon 16419, Republic of Korea

* E-mail: junghoyoon@skku.edu

† Contributed equally to this work



1 synapses to fully leverage neuromorphic computing.²⁸⁻³¹ Although 57
 2 conventional CMOS-based electronics have been used to develop 58
 3 artificial synapses and neurons as neuromorphic devices, they are 59
 4 limited by circuit area and energy efficiency.³²⁻³⁴ Since the CMOS 60
 5 based devices are optimized for digital switching, they struggle to 61
 6 handle smooth and continuous signal variations, which are essential 62
 7 for accurately reflecting external stimuli. Thus, essential functions 63
 8 such as the accumulation of external stimuli, the generation of 64
 9 corresponding output signals, and information storage inevitably 65
 10 performed by separate components. As a result, the emulation 66
 11 process compromises both area and energy efficiency in proportion 67
 12 to the number of devices used.³⁵ Moreover, implementing analog 68
 13 switching to achieve both the precision and dynamic range required 69
 14 for emulating biological counterparts remains a significant challenge 70
 15 in conventional CMOS-based systems. These systems necessitate the 71
 16 incorporation of additional circuitry, such as Digital-to-Analog 72
 17 Converters (DACs), to facilitate analog switching. Although more 73
 18 complex DAC configurations are required to enhance the output 74
 19 resolution, the resulting output often lacks the desired smoothness 75
 20. Meanwhile, among various neuromorphic devices, the memristor 76
 21 stands out for its area-efficient structure as well as high-speed and 77
 22 low-power operation. Additionally, their excellent scalability, 78
 23 durability, and uniformity make them well-suited for the reliable 79
 24 implementation of artificial sensory systems.³⁶⁻⁴⁰ Furthermore, 80
 25 unique attribute of memristors is their ability to gradually switch 81
 26 between a low-resistance state (LRS) and a high-resistance state 82
 27 (HRS) in response to external stimuli, such as voltage or current. 83
 28 In other words, memristors exhibit continuous and dynamic resistance 84
 29 state changes rather than relying on binary resistance states. This 85
 30 enables the direct processing of analog external stimuli without the 86
 31 complex configuration of using multiple devices or peripheral circuitry 87
 32 such as analog-to-digital converters. Therefore, the dynamic resistance 88
 33 switching provided by memristors is essential for replicating the 89
 34 artificial sensory system, as it more efficiently captures the high 90
 35 fidelity of incoming signals. Owing to these advantages, memristors 91
 36 have been widely utilized in the implementation of artificial 92
 37 receptors, synapses, and neurons.^{41, 42} In particular, their material 93
 38 composition, device structure, and switching dynamics can be 94
 39 carefully engineered to optimize switching behavior, making them 95
 40 adaptable to both volatile and non-volatile properties—key 96
 41 characteristics for mimicking biological elements.^{34, 43-51} The 97
 42 integrating memristive devices with various sensors facilitates the 98
 43 implementation of artificial sensory systems corresponding to 99
 44 tactile, visual, auditory, and olfactory modalities.^{52, 53}

45 In biological sensory systems, sensory receptors located in 100
 46 sensory organs convert external perceptual signals into receptor 101
 47 potentials, and sensory neurons integrate these potentials to initiate 102
 48 action potentials. Finally, the synapses store the encoded sensory 103
 49 information. Similarly, in a bioinspired memristive sensory system, 104
 50 sensors generally convert external stimuli into electrical signals 105
 51 which are then applied to memristors. Subsequently, the memristor 106
 52 receptor device that receives the signal generates a potential that is 107
 53 proportional to the input, incorporates information regarding 108
 54 harmful stimuli, and transfers it to the subsequent sensory system. 109
 55 Subsequently, the integrated memristive synapse and neural device 110
 56 respond to input signals in a manner analogous to biological

perception systems. By mimicking the biological sensory system, the 111
 integration of sensory, processing, and memory components in 112
 bioinspired memristive systems enables high power efficiency, low 113
 latency, and excellent processing capabilities.

Despite the versatility of memristors, current research has 114
 predominantly focused on signal conversion based on their switching 115
 characteristics. This approach has contributed immensely to the 116
 advancement of neuromorphic computing by enabling reliable and 117
 direct conversion of external stimuli into signals that drive neural 118
 networks implemented in hardware and software. However, studies 119
 on how closely these conversions align with the behavior of the 120
 human nervous system are lacking. The existing memristor-based 121
 systems often fail to fully capture the intricate dynamics of biological 122
 sensory systems, particularly in terms of complexity and adaptability. 123
 Devices capable of replicating the full range of functions of biological 124
 receptors, neurons, and synapses remain exceedingly rare. Even at 125
 the individual level, most artificial systems struggle to replicate all 126
 the critical functions of a single biological element. In artificial 127
 sensory systems, this limitation is further compounded by the 128
 frequent exclusion of specific functions or entire elements, resulting 129
 in incomplete or inefficient performance. This highlights a critical 130
 challenge: implementing all essential characteristics necessary for 131
 effective emulation. For artificial sensory systems to accurately 132
 process external stimuli across diverse environmental conditions, 133
 several crucial properties must be considered, including sensitivity, 134
 adaptability, and spatiotemporal processability. For instance, 135
 biological systems can dynamically adjust their sensitivity to external 136
 stimuli, such as by enhancing auditory perception in noisy 137
 environments or modulating visual processing under low light. 138
 Emulating this adaptability requires devices capable of self-tuning 139
 and learning in response to changing environmental conditions. 140
 Moreover, processing spatiotemporal patterns—similar to biological 141
 synapses responding to time-dependent signals—remains essential 142
 for replicating complex sensory functions. A systematic 143
 understanding of these properties is fundamental to developing 144
 artificial sensory systems that process complex input patterns with 145
 greater accuracy and efficiency.

In this review, the recent advances, challenges, and prospects of bio- 146
 inspired memristive artificial sensory systems are comprehensively 147
 examined. In this context, the switching performance metrics 148
 required for memristors in the implementation of artificial sensory 149
 systems, as depicted in Fig. 1, along with the sensory modalities they 150
 aim to emulate, are discussed. The subsequent sections first explore 151
 the fundamental roles of receptors, neurons, and synapses in 152
 biological sensory systems, along with the corresponding switching 153
 characteristics of memristors essential for replicating these neuronal 154
 components. Next, innovative cases of bio-inspired artificial sensory 155
 systems developed for the four primary senses—tactile, visual, 156
 auditory, and olfactory—are presented. Recent memristor research 157
 progress is then examined, focusing on how closely these systems 158
 mimic biological sensory functions and evaluating the effectiveness 159
 of these advancements. Finally, challenges and prospects for the 160
 development of memristor-based artificial sensory systems are 161
 addressed. This review aims to encourage ongoing research and



1 development, fostering a deeper understanding and broad
2 application of bio-inspired sensory systems by analyzing the roles
3 receptors, neurons, and synapses, the switching dynamics
4 memristors, and the necessary characteristics for each type of neuron
5 implementation.

6 2. Element of the nervous system: Receptor, 7 Neuron, and Synapse

8 To emulate the characteristics of receptors, neurons, and synapses
9 using memristors, a comprehensive understanding of their
10 operational mechanisms is required. Additionally, investigating the
11 switching properties of memristors and exploring how these
12 properties can be utilized to mimic each component are essential.
13 This process is crucial for precisely controlling the electrical
14 characteristics of memristors and effectively reproducing the
15 complex functions of the nervous system, as shown in Fig. 2.

16 2.1 Receptor

17 Receptors play a crucial role in detecting and responding to various
18 stimuli, enabling us to perceive and interact with the environment.
19 ⁵⁵ Receptors convert physical and chemical stimuli into electrical
20 signals. This process enables humans to appropriately respond
21 stimuli. Receptors have evolved to be specifically responsive
22 stimuli and can be classified into categories based on their ability
23 accommodate different external stimuli, such as mechanoreceptors,
24 thermoreceptors, photoreceptors, chemoreceptors, and
25 nociceptors.

26 Receptors operate based on thresholds and relaxation.⁵⁶ The
27 threshold indicates the minimum intensity of a stimulus required
28 be activated, below which the receptor remains unresponsive. This
29 characteristic enables the receptors to filter out insignificant minor
30 stimuli and focus on more critical signals. Upon activation by external
31 stimuli, receptors transition into a relaxed state where their
32 responsiveness to the stimulus gradually diminishes, enabling them
33 to revert to their initial state. During the relaxation state, receptors
34 retain a certain degree of activation; consequently, the threshold
35 intensity of the stimulus for reactivation is reduced compared with
36 that of the initial activation. This phenomenon, known as
37 sensitization, is crucial for modulating receptor sensitivity.
38 Additionally, some receptors exhibit adaptation characteristics
39 whereby their response diminishes in the presence of continuous
40 stimuli. These receptors provide essential protection against
41 persistent and harmful stimuli while also preventing energy
42 expenditure on non-essential stimuli.

43 The volatile memristor is suitable as an artificial nociceptor because
44 it reacts only to electric pulses above a certain threshold and
45 gradually reduces the output signal once the pulse is removed.^{58,59}
46 Moreover, such threshold and relaxation behaviors strongly depend
47 on the strength, period, and duration of the input signal. Regulation
48 relaxation enables the mimicry of phenomena observed in certain
49 receptors, such as allodynia, in which the threshold is lowered upon

exposure to harmful stimuli, and hyperalgesia, in which the response
is amplified. In addition, this approach enables the implementation
of adaptation functionality, which allows the receptors to adjust to
repeated stimuli. The detailed mechanisms and applications are
discussed in Section 3.

2.2 Neuron

Neurons constitute the fundamental units of the nervous system that
transmit electrical signals generated by external stimuli at receptors
in the brain, enabling recognition and response to these stimuli.^{61, 62}
Neurons are primarily composed of the cell body (soma), dendrites,
and axons. The soma acts as the metabolic and genetic center of the
neuron, housing the cell nucleus and supporting vital cellular
functions. Dendrites extending from the soma receive signals from
other neurons or sensory receptors, whereas axons transmit
electrical signals to other neurons and muscles. These electrical
signals are generated from rapid changes in the membrane potential
of the axon, known as the action potential.⁶³ When the action
potential reaches the axon terminal, neurotransmitters are released
into the synapse and subsequently interact with the dendrites of the
postsynaptic neuron. Synaptic transmission facilitates the formation
of complex neural networks that enable information collection,
integration, transmission, and coordination. Neurons are classified
based on their functions and characteristics. For instance, sensory
neurons detect external stimuli, such as light, sound, and
temperature, and transmit this information to the central nervous
system. Motor neurons carry commands from the central nervous
system to the muscles or glands. Interneurons function as
intermediaries, processing and relaying information between
sensory and motor neurons.

Volatile memristors are well-suited as artificial neurons due to their
ability to exhibit a steep current response exceeding a threshold
stimulus, followed by a decrease through volatile switching—closely
mimicking action potentials. Additionally, they effectively integrate
inputs from multiple channels and generate repetitive spike signals
with frequencies proportional to the combined input levels. During
signal generation, volatile memristors dynamically adjust their
responses based on input strength and frequency, efficiently
encoding continuous analog signals into spike trains—similar to
biological neurons. This adaptability enables differentiation between
weak and strong stimuli, replicating sensory adaptation mechanisms
in the human nervous system. Recent studies have demonstrated the
implementation of Hodgkin–Huxley (HH) and leaky integrate-and-
fire (LIF) model neurons using volatile memristors, further
highlighting their compatibility with biological neuron models. These
models leverage the ability of memristors to replicate essential
neuronal behaviors such as voltage-dependent conductance and
firing dynamics. Specifically, artificial neurons using volatile
memristors encode temporal information by adjusting their spiking
frequency based on the input intensity, closely resembling the time-
dependent stimulus information of biological sensory neurons.
Moreover, memristor-based implementations offer advantages such
as low power consumption and scalability while achieving
comparable performance to biological neurons.



- 1 **2.3 Synapse** 55 These findings demonstrate the ability to implement various forms
56 of synaptic plasticity and memory functions, highlighting their
57 potential suitability for efficient brain-inspired computing
58 architectures.
- 2 Synapses serve as junctions between the axon of one neuron and the
3 dendrite of another, playing an essential role in neural
4 transmission.^{52, 64} When an electrical signal reaches the axon of a
5 presynaptic neuron, the synapse adjusts the connection strength
6 (synaptic weight) based on the input signal, either strengthening or
7 weakening the synaptic weight. The dynamic regulation of synaptic
8 weight is fundamental to learning and memory and serves as a
9 critical component in understanding the functional mechanisms of
10 the human brain. Adjustments in synaptic weight, such as spike-
11 timing-dependent plasticity (STDP), short-term plasticity (STP), and
12 long-term plasticity (LTP), are fundamental to the ability of the brain
13 to adapt, learn, and form memories.⁶⁵⁻⁶⁷ STDP is used to effectively
14 control synaptic weight, demonstrating a type of synaptic plasticity
15 that depends on the exact timing between the two neurons. This
16 mechanism facilitates the efficient utilization of neural networks by
17 leveraging the temporal interactions between neurons. STP refers to
18 temporary changes in synaptic strength. The STP lasts from a few
19 seconds to several minutes and can fluctuate based on the activity
20 patterns of the neurons. It is primarily governed by intracellular
21 mechanisms associated with neurotransmitter release and plays a
22 crucial role in adapting to rapidly changing environments and
23 processing transient information. Unlike STP, LTP is required for long-
24 term memory formation. LTP refers to the sustained enhancement
25 of synaptic strength over extended periods, ranging from hours to
26 years. It is known to play a critical role in learning and memory
27 processes and arises from the repeated activation of specific neural
28 paths.
- 29 Non-volatile memristors are highly suitable for mimicking synaptic
30 characteristics.^{59, 68, 69} Non-volatile memristors exhibit resistance
31 changes in response to electrical stimuli, effectively replicating the
32 synaptic weight. Furthermore, the switching behavior of non-volatile
33 memristors, which allows them to retain information even in the
34 absence of a bias, enables the emulation of long-term memory
35 functionality. The modulation of resistance and synaptic weight
36 assumes a critical function for assessing the intensity of previous
37 input signals within the frameworks of machine learning and neural
38 network algorithms. The linearity of resistance modulation is crucial
39 and can be effectively utilized to deduce the strength of the signals.
40 Linearity is essential for improving the precision of the numerous
41 algorithms used in machine learning and neural networks.
42 Furthermore, the potential of utilizing non-volatile memristors
43 emulate the characteristics of synaptic devices has been
44 demonstrated, enabling the replication of various forms of synaptic
45 plasticity such as LTP, STP, and STDP. In detail, non-volatile
46 memristors can exhibit STDP behavior, where synaptic strength is
47 modified based on the timing of pre- and post-synaptic input spikes.
48 In addition, LTP and STP can be achieved by adjusting the device
49 conductance in response to varying input frequencies, allowing non-
50 volatile memristors to adapt to both transient and sustained input
51 patterns. This is achieved through the precise control of the
52 formation of conductive pathways, which are closely associated with
53 resistance changes in non-volatile memristors. This approach
54 effectively reproduce the dynamic properties of synaptic plasticity.

3. Memristor-based tactile sensory system

Human skin enables us to recognize objects and interpret the environment through the sense of touch. Tactile perception is complex and involves sensing, refining, learning, and forming interactions with the external environment.⁷⁰⁻⁷³ Receptors on sensory neurons embedded in the skin, such as nociceptors, chemoreceptors, and mechanoreceptors, detect various somatic sensations and convey tactile information to the brain via electrical signals. This process enables exquisite sensations of object recognition, texture discrimination, and sensory feedback. Tactile receptors can detect even small amounts of pressure or force, and when combined with external stimuli, they provide a detailed and nuanced picture of the object or surface being touched. This information can help humans navigate their environment, manipulate objects, and perform tasks that require a sense of touch. They can also improve the functionality and comfort of prosthetic limbs by providing users with a more natural and intuitive sense of touch. This chapter explains memristor-based electronic tactile sensory systems related to somatic sensations.

3.1 Memristor-based nociceptor and adaptive receptor

Nociceptors play a vital role in mimicking human acceptance and processing of external stimuli. When a stimulus such as mechanical stress, chemical stress, or temperature is applied, the nociceptor determines the degree of hazard and generates the corresponding biochemical signals. Therefore, to assess the danger posed by external stimuli and to respond to and safeguard oneself, all diverse features must be incorporated into the nociceptor.^{74, 75}

Memristor-based nociceptors are similar to bionociceptors in that they respond differently to different stimuli. As shown in Fig. 3a, Yoon et al. established an artificial nociceptor based on an Ag-based threshold-switching memristor with the function of a nociceptor that implements four key functions (threshold, relaxation, no adaptation, and sensitization).⁷⁶ Allodynia and hyperalgesia, resulting from harmful or abnormal stimuli, can be effectively induced in memristors by applying high voltages that exceed the threshold level. When the input voltage is increased to a level perceived as harmful, the conductive paths in the memristor grow excessively, making spontaneous and complete rupture challenging after the voltage is removed. Consequently, residual Ag clusters or conductive paths remain within the oxide film, facilitating a rapid response to stimuli below the threshold (sensitization). To further demonstrate the potential of the nociceptor, an artificial Ag-based nociceptor memristor was integrated into the thermoelectric module. The thermal nociceptor only generated an electric spike at a critical temperature (50 °C, hazardous temperature). As the temperature increased, the signal amplitude increased, and the onset time decreased.





1 Kim et al.⁷⁷ reported an artificial nociceptor based on a Pt/HfO₂/TiN
 2 memristor utilizing trap/detrapping mechanisms instead of a cationic
 3 based threshold-switching memristor. The nociceptive function was
 4 imitated by adjusting the trap depth of the HfO₂ layer. When
 5 sufficiently high positive voltage was applied to Pt, lowering the trap
 6 level below the Fermi energy level of TiN facilitated electron injection
 7 from TiN to fill the trap sites. Once filled, the electron transport
 8 increased sharply due to trap-assisted tunneling conductivity
 9 between trap sites, turning the device on (threshold switching). After
 10 the voltage was removed, the difference in work functions between
 11 the Pt and TiN electrodes created a built-in potential that caused the
 12 trapped electrons to relax over time (relaxation). The device
 13 exhibited a wide operation time span ranging from milliseconds to
 14 ten seconds, with a relaxation time scale well-matched to typical
 15 biological systems making it highly effective for mimicking nociceptor
 16 behavior. Therefore, additional circuits have been designed to
 17 effectively mimic biological reflex actions, enabling immediate
 18 response generation and transmission to the spinal cord when
 19 exposed to danger.

20 There is an increasing need for humanoid robots to imitate advanced
 21 biological functions to respond efficiently to external environment.
 22 Biological skin can protect itself against harmful damage by detecting
 23 the degree of danger and initiating appropriate actions using
 24 nociceptors. Moreover, biological skin can self-heal and eventually
 25 return to its normal state when damaged by external stimuli. The
 26 design of a memristor is crucial for mimicking the complex
 27 characteristics of bioskin. Xiaojie et al. reported an artificial sensory
 28 system with the ability to sense and warn patients of pain and heal
 29 itself. The FK-800-based organic volatile memristor acted as an
 30 electronic skin (Fig. 3b).⁷⁸ Self-healing was achieved because of the
 31 intrinsic characteristics of the organic material, similar to human
 32 skin. In addition, to sense pain and signs of injury, the artificial tactile
 33 system was composed of a triboelectric generator, volatile
 34 memristor, and light-emitting diode (LED). The triboelectric
 35 generator and volatile switching memristor act as mechanoreceptors
 36 and nociceptors, respectively. The triboelectric generator generates
 37 an output voltage based on the intensity of the external stimulus,
 38 and the generated voltage is applied to a volatile memristor. When a
 39 voltage above the threshold value was applied to the volatile
 40 memristor, the memristor and LED turned on. This case was
 41 considered to have minimal damage or pain and was not considered
 42 a threat. When a voltage below the threshold value was applied, the
 43 memristor and LED did not turn on, causing no damage or pain.
 44 Conversely, when a large input voltage was applied to the memristor
 45 as a strong stimulus, the relaxation time and resistance of the volatile
 46 memristor were longer and lower, respectively. Therefore, the LED
 47 was stronger and required a longer time to turn off completely.

48 To effectively perceive the external environment, it is essential to
 49 recognize both harmful and incoming nonharmful stimuli.
 50 Nociceptors react to potentially harmful stimuli such as pressure,
 51 heat, or chemicals, transmitting signals to the brain, where they are
 52 interpreted as pain. They respond consistently to specific types of
 53 stimuli (no adaptation). In contrast, adaptive receptors reduce their
 54 sensitivity when exposed to continuous stimulation (adaptation).

facilitating the filtration of unimportant and repetitive information.⁷⁹
 80 This mechanism is essential for sensory processes such as vision,
 hearing, and touch, allowing humans to adjust to dynamic
 surroundings.

However, its implementation is difficult for both the existing CMOS-
 based and memristor-based receptors. Song et al. proposed an
 artificial receptor that mimicked both the adaptive and maladaptive
 characteristics using an Ag-based volatile memristor.⁸¹ The artificial
 receptor was implemented by adjusting the thickness of the
 conductive filament with varying amounts of metal ions. The
 competitive relationship between Joule heating and
 electromigration was controlled by the number of metal ions, which
 determined the thickness of the conductive filament. Fig. 3c shows
 that the thin conductive filament (low Ag concentration) ruptured
 due to Joule heating during high-intensity stimuli (adaptive
 receptor), whereas the thick filament (high Ag concentration)
 maintained an electrical on-state (maladaptive receptor). Thus, the
 authors demonstrated the feasibility of implementing normal
 sensory-receptor behaviors.

3.2 Tactile stimulus perception

Artificial electronic skin, which captures surrounding tactile stimuli,
 is deployed in advanced intelligent systems. Conventionally, artificial
 electronic skin requires additional external equipment to store and
 process large amounts of data. However, this structure is inefficient
 in terms of energy consumption and processing speed because it
 causes time delays and large energy consumption. Memristor-based
 tactile sensory systems can effectively emulate the functions of
 human tactile nerves in low-power operations without requiring
 additional equipment. Memristor-based tactile sensory systems
 enable the recording of stimuli by translating external mechanical
 stimuli into modulated electrical spikes. To mimic a tactile sensory
 system, an artificial system generally comprises a bio-inspired
 synaptic or neuron memristor and various sensors for detecting the
 external environment. The sensor connected to the memristor
 detected the strength of the external stimulus and generated various
 electrical signals based on the degree of stimulation applied. The
 memristor integrates the output signals of the parallel sensor and
 processes them into unified electrical spikes.⁸²⁻⁸⁴

Wang et al.⁸⁵ demonstrated an ultrafast artificial skin system based
 on near-sensor analog computing architecture. The artificial skin was
 implemented by combining a memristor with a tactile sensor and
 was fabricated on a flexible substrate. When a tactile sensor
 recognizes an external stimulus, an input pulse is generated and
 applied to the memristor to alter its resistance. Accordingly, the
 system simultaneously captures and processes the tactile stimuli in
 real time. In addition, the authors suggested that the system could
 be mounted on a finger or prosthesis to detect the edge information
 of external objects in real-time (Fig. 4a).

Sensory systems can simultaneously receive and transmit various
 types of information from the environment via various receptors.
 Similar to human reliance on multiple stimuli for decision-making

1 and responses, artificial nervous systems that utilize memristors 54
 2 require the integration of information from diverse external stimuli 55
 3 to achieve effective functionality. Artificial sensory systems aim 56
 4 to achieve multisensory functions by simultaneously integrating and 57
 5 processing various sensory input signals. The first approach involves 58
 6 integrating the input signals obtained from a circuit comprising 59
 7 multiple sensors and a memristor. Xinqiang et al.⁸⁶ developed 60
 8 a multimodal sensory system that utilized pressure and temperature 61
 9 sensors in conjunction with non-volatile memristors and employed a 62
 10 signal coupling method to integrate the outputs (Fig. 4b). The input 63
 11 stimulus can be integrated from different sensors, and an output 64
 12 signal can be generated once the input signal from each sensor 65
 13 reaches a fixed threshold voltage. Six pressed and two hot stimuli 66
 14 were applied to the system, which recognized eight stimuli and 67
 15 generated an eight-fold output. Correspondingly, the memristor 68
 16 reacted to several toxic stimuli and modulated conductance. This 69
 17 study demonstrates that a multimodal artificial sensory system can 70
 18 be constructed using different sensors (pressure and temperature) 71
 19 and signal-coupling modules. 72
 20 A multimodal sensory system can be realized using memristor 73
 21 materials. This approach simplifies the circuits that constitute the 74
 22 multimodal sensing, making it efficient and advantageous in terms of 75
 23 energy utilization. Qingxi et al. developed a multisensory system by 76
 24 configuring an oscillation circuit using piezoresistive sensors and a 77
 25 VO₂-based volatile memristor (Fig. 4c).⁸⁷ VO₂ exhibits inherent 78
 26 thermal sensitivity, which enables its resistance state and 79
 27 characteristics to change in response to temperature fluctuations. 80
 28 Consequently, the VO₂-based memristor enables the monitoring of 81
 29 temperature stimuli without the need for supplementary sensors. 82
 30 When direct thermal stimuli are applied to a memristor, the inherent 83
 31 thermal sensitivity characteristics of VO₂ alter the switching behavior 84
 32 thereby inducing a change in the oscillation circuit characteristics. 85
 33 In addition, when haptic actions are applied to a piezoresistive sensor, 86
 34 the magnitude of the stimulus alters the output of the sensor, which 87
 35 in turn changes the voltage applied to the non-volatile memristor, 88
 36 consequently modifying the oscillation characteristics of the volatile 89
 37 memristor. Therefore, without multiple sensors or electrical modules, 90
 38 an artificial mechanical sensory system can effectively synchronize 91
 39 information regarding external stimuli through vibrations that vary 92
 40 in response to pressure and temperature. 93
 41 Memristor-based tactile receptors effectively detect various external 94
 42 stimuli, including heat and pressure. These receptors mimic the 95
 43 ability to recognize external stimulus patterns and generate 96
 44 appropriate responses through sensor integration and 97
 45 computational analyses. However, sensor integration remains 98
 46 energy inefficient, and research on their ability to process multiple 99
 47 stimuli simultaneously remains limited. Further investigation 100
 48 needed on software-based approaches for classifying and analyzing 101
 49 simultaneous stimuli, such as applying algorithms similar to the 102
 50 single-coupling module shown in Figure 4b. These additional 103
 51 approaches can enhance the accuracy of human tactile system 104
 52 emulation. 105

53 **4. Memristor-based visual sensory system**

Human vision is the primary method used to assess the size, shape, 106
 color, brightness, distance, and surface roughness of an object. 107
 Humans acquire more than 80% of their external information 108
 through the visual sensory system. In the information acquisition 109
 process, the eyes, brain, and muscles collaborate to perceive light 110
 stimuli and protect oneself by responding to potentially harmful 111
 stimuli.⁸⁸⁻⁹⁰ The human visual sensory system rapidly processes these 112
 complicated tasks in a highly accurate and energy-efficient manner. 113
 Thus, mimicking this system is desirable for the efficient detection, 114
 processing, and storage of large volumes of visual information. 115
 However, the biological visual system features a complex hierarchical 116
 organization, including neural structures, such as the retina, bipolar 117
 cells, horizontal cells, and ganglion cells. Consequently, mimicking 118
 this system by using electronic circuits requires highly complex 119
 circuits and substantial energy consumption for information 120
 processing. Therefore, the development of more compact and 121
 efficient artificial visual sensory systems that can integrate sensing, 122
 processing, and storage functions is required. In Section 3, we 123
 describe a method that mimics human visual characteristics, such as 124
 light and motion detection, and the perception of an object using a 125
 memristor. This approach employs a memristor to mimic the visual 126
 adaptation functions, enhance efficiency, and reduce the complexity 127
 of an artificial visual system.

4.1 Retina-like preprocessing

The retina contains photoreceptors that detect external stimuli and 128
 transmit visual data to bipolar cells, which serve as intermediaries 129
 between the photoreceptors and ganglion cells. The data are then 130
 relayed through synapses with ganglion cells, triggering action 131
 potentials that travel to the lateral geniculate nucleus (LGN). The LGN 132
 transmits these signals to the visual cortex. In this process flow, a 133
 memristor can process information related to light intensity, directly 134
 detect the light intensity, or appropriately adapt to changes in the 135
 ambient light levels of the external environment.^{91, 92}

Dang et al.⁹³ demonstrated that the one-phototransistor-one- 136
 memristor (1PT1R) synaptic device shown in Fig. 5a has the potential 137
 for in-sensor computing and edge computing in visual sensory 138
 systems. In the 1PT1R structure, the ZnO-based phototransistor 139
 provides a driving current proportional to the light illumination, 140
 enabling the implementation of a high-linearity light-tunable 141
 multilevel conductance state within the Mo/SiO₂/W memristor. 142
 Moreover, an optical artificial neural network (OANN) composed of 143
 a 16 × 3 1PT1R array performs cross-talk-free conductance updates 144
 because the phototransistor functions as a selector. The proposed 145
 OANN achieved a 99.3% accuracy in image recognition, 146
 demonstrating that the 1PT1R device is a promising hardware 147
 solution for artificial visual systems.

Shan et al.⁹⁴ demonstrated fully light-modulated synaptic plasticity 148
 using a plasmonic optoelectronic memristor comprising Ag 149
 nanoparticles embedded in a TiO₂ nanoporous film. Fig. 5b illustrates 150
 the photooxidation and reduction processes of the Ag nanoparticles 151
 embedded in the device under UV/Vis irradiation. Under visible light 152
 irradiation, electrons from Ag transferred to the conduction band of



1 the TiO₂ film, generating Ag⁺ ions. This increased the effective
 2 diameter of the Ag conducting filament, thereby enhancing device
 3 conductivity. In contrast, UV irradiation excited electrons in the
 4 valence band of the TiO₂ film to its conduction band, which reduced
 5 the number of Ag⁺ ions and suppressed the increase in device
 6 conductivity. Consequently, when electrical pulses were applied
 7 after UV and visible-light irradiation, the current response was
 8 greatly improved only under visible-light irradiation. This enables the
 9 emulation of light-induced and gated synaptic plasticity. The STP
 10 learning was conducted using UV/Vis light. The memristor effectively
 11 eliminates image noise owing to its specific UV light-induced long-
 12 term depression (LTD) function. In addition, light-induced STP
 13 learning has been identified as a feature of high-level image
 14 processing. By incorporating low-level image preprocessing steps
 15 such as contrast enhancement and noise reduction, the learning rate
 16 and efficiency of high-level image recognition processes can be
 17 significantly improved by these memristors, as demonstrated
 18 through simulations.

19 Xu et al.⁹⁵ reported the HH neuron-based artificial visual sensory
 20 system shown in Fig. 5c using a volatile VO₂ memristor. The volatile
 21 VO₂ memristor modulates the threshold and hold voltages based on
 22 temperature, which mimics a biological neuron. The proposed
 23 volatile memristor exhibits frequency relaxation in tonic spiking
 24 type of neuron spiking model) under varying pulse inputs, and
 25 transition between spiking models when the input pulse changes
 26 abruptly. This is analogous to the light-adaptive functions of
 27 photoreceptors (cone and rod cells) in the retina. Primary
 28 photoreceptors responsible for light processing change during the
 29 transition between bright and dark environments. This shift, referred
 30 to as photopic and scotopic adaptation, has been successfully
 31 realized in a circuit comprising an HH neuron, a thermoelectric
 32 ceramic, and a light-dependent resistor. These components convert
 33 light into thermal stimuli that are subsequently used to generate
 34 input pulses that induce frequency changes during spiking. This light-
 35 adaptable function is useful for artificial applications. The authors
 36 demonstrated the potential of integrating spiking neural network
 37 (SNN) algorithms into machine vision applications to simplify circuit
 38 and complex processing.

39 4.2 Self-protection via detecting the intensity of light

40 In addition to light detection, the visual system should also be
 41 capable of analyzing the diverse spatiotemporal patterns of
 42 photoreceptors activated in the retina. This involves protective
 43 behaviors such as closing the eyes to shield against damage from
 44 intense light and impending collisions, and nociceptive functions to
 45 detect harmful light stimuli.

46 A highly efficient artificial visual sensory system comprising an
 47 optoelectronic threshold-switching memristor and an actuator was
 48 proposed by Pei et al.⁹⁶ The Sb₂Se₃/CdS-core/shell nanorod array-
 49 based (SC) optoelectronic memristor enhanced light-harvesting
 50 activities, received optical signals, and converted them to a voltage
 51 before transmitting them to the threshold-switching memristor-
 52 based neuron circuit. The SC memristor exhibited resistive switching

characteristics in a light-irradiated environment, as shown in Fig. 6a,
 driven by conductive dangling bonds and vacancy defects on the
 surface of the Sb₂Se₃ nanorods. This results in an increased ON/OFF
 resistance ratio, which in turn increases the firing frequency of
 neuronal circuits proportional to the light intensity. When the light
 exceeded the safety range, the firing frequency and amplitude of the
 SC memristor and neuron circuit increased significantly, potentially
 triggering an electric actuator. This emulates eye muscle contraction
 and reproduces the self-protective behavior of closing eyes in
 response to intense light damage.

Wang et al.⁹⁷ developed an artificial visual sensory system motivated
 by locusts, which, compared to humans, have a superior perception
 of moving objects. The vision system of locusts includes a lobular
 giant movement detector (LGMD) that generates danger signals
 before the occurrence of collisions. This functionality is
 demonstrated in Fig. 6b using an Ag conductive filament-based
 threshold-switching memristor. The formation and rupture of Ag
 conductive filaments in the volatile memristor were used to
 implement the excitatory and inhibitory effects on LGMD neurons.
 The conductivity of the volatile memristor increased and then
 decreased as the intensity of light increased. When the light power
 applied to the device was gradually increased to correspond to the
 approaching objects, the current response initially increased,
 reached a peak, and then decreased as the collision point
 approached. In detail, at low light intensities, moderate Joule heating
 accelerates the drift of Ag⁺ ions and the formation of conductive
 filaments, while at high light intensities, significant Joule heating
 induces the rupture of Ag conductive filaments. Consequently, the
 LGMD neuron implemented in this configuration provides
 information prior to the collision point, enabling self-protective
 behavior.

Li et al.⁹⁸ demonstrated a visual nociceptor based on a two-terminal
 optical synaptic device with a monolayer MoS₂ depicted in Fig. 6c.
 The optical synaptic device successfully emulated adjustable synaptic
 behaviors, including STP, LTP, and paired-pulse facilitation (PPF), by
 leveraging the persistent photoconductivity resulting from charge
 trapping. Notably, when the device was stimulated with light
 intensities ranging from 2.5 to 7.5 nW/μm², the photocurrent
 reached a higher level of saturation, which aligned with the no-
 adaptation characteristic of nociceptors. Furthermore, when paired
 320 nm light pulses were applied to the optical synaptic device at
 intervals of 1, 2, and 3 s, a stronger photocurrent was observed at
 shorter intervals, demonstrating the dependence of the device on
 the relaxation time. Additionally, ultraviolet pulses with a
 wavelength of 320 nm and power densities of 25 and 75 nW/μm²
 were used to induce low-injured and strong-injured states,
 respectively. In these injured states, the device exhibited a
 heightened sensitivity to light pulses. In the low-injured state, even a
 low-intensity ultraviolet pulse (1.5 nW/μm², 1 s) exceeded the
 activation threshold, while in the strong-injured state, an intensity of
 1.2 nW/μm², which is below the threshold, produced a significant
 photocurrent. This behavior mirrors the nociceptor characteristics of
 "allodynia" and "hyperalgesia," where sub-threshold stimuli can
 elicit a response in an injured state.



1 To implement artificial visual sensory systems, memristors have been
 2 integrated with separate photodetection devices or fabricated using
 3 photoresponsive materials. While integration with separate devices
 4 ensures reliable processing of external stimuli, photoresponsive
 5 memristors offer superior integration density. However, incorporating
 6 photodetection capabilities into memristors often requires additional
 7 fabrication steps, such as coating nanorod arrays with photoactive
 8 materials or using ultrathin channel materials like nanosheets, which
 9 increases complexity. Therefore, further research is required to develop
 10 simplified fabrication techniques for photoresponsive memristors.

12 5. Memristor-based auditory sensory system

13 The biological auditory system detects and collects information from
 14 pressure waves of different amplitudes, frequencies, and components
 15 in the medium generated by motion or collision. Sound waves that arrive
 16 at the ear are mechanically transmitted to sensory hair cells in the
 17 cochlea, generating amplified electrical signals owing to mechanical
 18 vibrations. Information in the form of amplified electrical signals is
 19 transmitted from the auditory sensory nerves to the cerebral cortex.
 20 Through this process, humans recognize sounds in their surroundings.
 21 The input sound is encoded as a train of electrical pulses created from
 22 the output of a frequency-selective channel in the cochlea (space-to-
 23 rate encoding). Sparse sampling of the frequency information was
 24 performed according to the active frequency channel without capturing
 25 all information from the sound source at the maximum sampling rate.
 26 Using this coding strategy, the cerebral cortex efficiently extracts key
 27 information from complex sound signals, enabling the biological auditory
 28 system to produce higher-level perceptions including sound location,
 29 rhythm perception, pitch recognition, and sound recognition. The ear
 30 receives a combination of simultaneous sound sources with various
 31 frequency components. This complexity is further exacerbated because
 32 both the frequency and amplitude of these components can be converted
 33 into a single sound. Owing to the spatiotemporally encoded nature
 34 and time dependency of sound waves, signal processing in the auditory
 35 system is more complicated than that in the visual or tactile systems.
 36 Chapter 4 introduces the pioneering demonstration of an integrated
 37 memristor-based artificial auditory system divided into sound location
 38 (azimuth detection) and sound recognition.

41 5.1. Sound location

42 To determine the location and direction of a sound source, the
 43 human brain relies on interaural time difference (ITD), which is the
 44 difference in the time of sound arrival between the two ears. The
 45 sound signal is generally divided into a left and right signal to be
 46 processed, and the important clue for sound location is the ITD in the
 47 range of -0.6 ms to 0.6 ms. Based on ITD theory, several successful
 48 demonstrations of sound localization have been conducted using
 49 memristors.

50 To emulate sound localization based on the ITD, Sun et al.¹⁰²
 51 demonstrated precise temporal computation for the identification of

acoustic sound locations using the intrinsic synaptic capability of
 short-term synapses. Based on the Joule heating and versatile
 doping-induced metal-insulator transitions in a scalable monolayer
 MoS₂ device, synaptic computation was conducted to process a given
 acoustic signal, as shown in Fig. 7a. The memristor device was
 designed with a biologically comparable energy consumption (10 fJ),
 and tunable STP was demonstrated by the flexible doping level of
 MoS₂. A circuit with this tunable synaptic device achieved ITD
 detection, emulating precise temporal computations in the human
 brain by suppressing the sound intensity- or frequency-dependent
 synaptic connectivity.

The integration of piezoelectric micromachined ultrasound
 transducer (pMUT) sensors into a neuromorphic RRAM-based
 computational map has been reported to demonstrate real-world
 sensory processing in object localization.¹⁰³ As shown in Fig. 7b,
 an event-driven auditory processing system applied to object
 localization was developed using an in-memory computing
 architecture. Inspired by the neuroanatomy of the barn owl, which
 is known to be an efficient auditory localization system with hunting
 capabilities during the night, the time-of-flight (ToF) of the sound
 wave was encoded, and the difference between the two ToF
 measurements (ITD) was analyzed to identify the sound location.
 The energy efficiency of object localization was realized by exploiting
 event-driven RRAM-based neuromorphic circuits that processed the
 signal information produced by the embedded sensors to calculate
 the position of the target object in real time. Unlike conventional
 sensory systems that continuously sample and calculate the detected
 signal to extract useful information, this energy-efficient auditory
 system performs asynchronous computations as useful information
 arrives.

Moreover, with the integrated 1 K HfOx-based analog memristor
 array and a multithreshold update scheme, the in situ learning ability
 of the sound location function was demonstrated.¹⁰⁴ As shown in
 Fig. 7c, a brain-like learning algorithm and architecture for the sound
 location function were successfully realized, demonstrating the
 capability of processing sound signals from two artificial ears. With
 high accuracy (45.7%) and energy efficiency (184 \times) compared to
 existing methods, it demonstrated a significant advancement toward
 realizing advanced auditory localization systems.

91 5.2. Speech recognition

92 Speech recognition, a key requirement for artificial intelligence
 machines to communicate with humans, has been widely developed
 in software-based neural networks. However, the long latency and
 large storage requirements for large amounts of voice data in speech
 recognition tasks in the existing von Neumann architecture pose
 limitations. Therefore, energy-efficient neuromorphic computing
 systems have a significant potential for processing audio signals.
 In this subsection, several memristive-based artificial auditory systems
 with highly accurate and efficient speech recognition performances
 are presented.



1 A TiN/HfO_x/TaO_x/TiN memristor device that features a multilevel
2 analog resistive state was developed.¹⁰⁵ The artificial cochlea-based
3 circuit was used to experimentally demonstrate the filtering
4 behaviors of five channels with different central frequencies.
5 Consequently, when connected to a convolutional neural network
6 as shown in Fig. 8a, it achieved the extraction of speech features,
7 demonstrating the feasibility of a highly efficient artificial cochlea
8 system.

9 An artificial van der Waals hybrid synapse was developed and
10 demonstrated using acoustic pattern recognition. Its superior
11 conductance controllability was achieved using WSe₂ and MoS₂
12 hybrid channels, which are specialized for linear and symmetric
13 conductance change characteristics.¹⁰⁶ The hybrid synaptic device
14 was used to perform acoustic pattern recognition (from recording,
15 transforming, and integrating) with high accuracy (93.8%), as shown
16 in Fig. 8b, indicating its potential for brain-inspired computing.

17 Speech recognition using a memristor array (W/MgO/SiO₂/Mo) with
18 multilevel conductance has also been demonstrated (Fig. 8c).
19 Speech recognition in a memristive SNN was achieved by precisely
20 tuning the weights of the artificial synapses. For effective and sparse
21 spatiotemporal feature extraction, a one-dimensional self-organizing
22 map (SOM) network was used, which essentially operated to achieve
23 high performance and simplify the SNN classifier. Compared to other
24 ANN-based systems, the advantages of a simplified structure and
25 high energy efficiency have been demonstrated in memristive SNNs
26 for speech recognition tasks.

27 Memristors have demonstrated excellent performance in converting
28 acoustic signals into electrical signals for artificial auditory sensor
29 systems. However, a significant portion of the processing, such as
30 post-processing and learning of the converted signals, still relies
31 heavily on software-based computations and simulations.
32 Additionally, there is potential for applications that can reduce
33 sensitivity or block sounds in response to sudden loud noises, but
34 further research is needed to explore and develop these possibilities.

35 6. Memristor-based olfactory sensory system

36 The integration and coordination of the olfactory receptors, cortex,
37 and muscles enables humans to recognize and memorize odor
38 stimuli and respond to specialized gases. In the biological olfactory
39 sensory system, odorants from the environment are detected by
40 olfactory receptors, which trigger electrical signals as the output.
41 Spike signals are generated by the olfactory sensory neurons and
42 transmitted through the olfactory bulb, where signal preprocessing
43 is performed. Finally, the preprocessed signals are transmitted to
44 higher regions of the brain (olfactory cortex) to identify and
45 memorize odors.¹⁰⁸⁻¹¹² Among the various perceptions, olfaction is
46 particularly complex and vague because of the complexity of the
47 chemosensory system, which must distinguish and quantify gas
48 molecules in constantly changing environments. Therefore, these
49 olfactory processes can provide information on complex smells,
50 which in turn can provide key guidance for awareness, decision-
51 making, and action in the surrounding environment.

Despite the importance of the olfactory system, relatively few
studies have been conducted because of its complexity. It remains a
challenge to completely emulate the functions of the human
olfactory system in recognizing, memorizing, and inducing muscle
movements in response to dangerous gases. Section 6 introduces
various artificial olfactory systems based on the functions of the
human olfactory system, including odor recognition, memorization,
and protection in dangerous and gaseous environments.

6.1. Odor recognition and memorization

The olfactory system, comprising thousands of different types of
receptors and classifiers, enables humans to recognize and
memorize odors. Stimulated by odorant molecules, specific spikes
are generated by the olfactory receptors and analyzed using neural
networks. Following learning and training, humans recognize
different odors through memorization using olfactory systems.
Although various strategies have been proposed to construct
artificial olfactory systems, most studies have focused on developing
systems that use gas sensors and complex neural networks. Recently,
a bioinspired memristor-based olfactory system with perceptual
learning and memorization abilities was developed to classify several
different gases.

Qifeng Lu et al. developed a hybrid flexible gas-detection system
utilizing NiO nanowall-based gas sensors, oscillators, and graphene-
based memristor-based synapses. In this system, the signals
generated by the gas sensor are converted into pulses by an
oscillator, and the frequency of these pulses varies based on the
resistance of the gas sensor. The stimulation of H₂S gas at various
concentrations was converted into pulse signals.¹¹³ The altered
pulses became presynaptic signals transmitted to the synaptic
devices, resulting in changes in the resistance (synaptic weight) of
the graphene-oxide-based synapse memristor. Resistance
modulation influences information processing and storage using
synaptic memristors. The system implements learning capabilities
based on the k-nearest neighbor (KNN) algorithm, which efficiently
categorizes unknown gas stimuli into the most probable categories
by comparing them with pre-learned boundaries. The gas-detection
system demonstrated enhanced recognition capabilities through
iterative learning. Initially, the error rate exceeded 45%; however, as
the number of learning iterations increased, the error rate
progressively decreased to approximately 20%. This methodology
enhances the practical application of gas-detection systems and
ensures reliable data analysis.

In addition to the mere recognition of a single gas, olfactory systems
have been reported to enable the detection of various gases.¹¹⁴ The
reported system utilizes an array of gas sensors along with neurons
and synapses to form an olfactory sensory system capable of
effectively analyzing complex gaseous environments. An array of gas
sensors capable of detecting four different gases (formaldehyde,
ethanol, acetone, and toluene) at various concentrations was used
to effectively monitor diverse gaseous environments. In a gaseous
environment, the resistance changes in each sensor adjusted the
intensity of the voltage applied to the series-connected neuronal



memristor (Pt/Ag/TaO_x/Pt) (Fig. 9a). These modifications to the input voltage translate the chemical information of the gases into electrical spikes in the neuron memristors, thereby providing information on the gas-detection capabilities of the entire system. The spikes generated in each neuron are transmitted to a synaptic array (Pt/Ta/TaO_x/Pt), where they undergo learning and training through spike rate-dependent plasticity (SRDP). This process enables the storage of gas characteristics in memristor devices. Based on matrix-vector multiplication, the system can effectively classify 100 different types of gases. This system enables the precise identification and quantification of gases with distinct chemical properties, which is highly beneficial for environmental monitoring. Furthermore, these memristor-based sensory systems overcome efficiency problems encountered in existing artificial sensory systems, such as frequent sampling, data storage, and transfer. Han et al. reported that sensors with differing sensitivities to the same gas were serially connected to memristor-based neurons, proposing an olfactory system capable of clearly recognizing and differentiating mixed gases.¹¹⁵ In this system, gas exposure alters the resistance of the gas sensors, modifying neuronal frequency, which can be used for gas detection. Sensors based on SnO₂ and WO₃ exhibit different resistance changes in response to the same gas, leading to distinct neuronal firing frequencies. This configuration enables the artificial olfactory system to distinguish unknown gases more accurately. Furthermore, integration with SNNs has enhanced the ability of the system to identify various types of reducing gases (NH₃, CO, acetone, NO₂). The introduction of additional hidden layers in the SNNs further improves the recognition of more complex gas mixtures, highlighting its potential for environmental monitoring and safety applications.

Currently, gas recognition and memory require additional gas sensors and circuits, which adversely affect the power consumption and miniaturization of the device. Chun et al. reported a system capable of recognizing and remembering gases without requiring additional devices or circuits by employing materials in synaptic memristors that exhibited both gas-detection capabilities and resistive change properties, as depicted in Fig. 9b. A synaptic memristor based on Pt/TiO₂ NR/TiN can directly detect gases and remember them through changes in the resistance state.¹¹⁶ The TiO₂ material, the oxide layer of synaptic devices, is not only used for resistive switching in synaptic memristors but is also employed for gas detection in conventional gas sensors. When a synaptic memristor is exposed to H₂ gas, the gas reacts with TiO₂ to generate oxygen vacancies, promoting the growth of conductive paths and decreasing resistance. Conversely, exposure to NO gas removes oxygen vacancies, causing disruptions in conductive paths and increasing the resistance. The synaptic device detects changes in resistance due to gas exposure and stores information regarding the exposure. This process enables accurate recording of information related to gas detection and provides reliable environmental monitoring. This technology plays a crucial role in measuring and managing gas concentrations in various environments. In addition, the gas detection capability of a single memristor can be effectively applied to mixed-gas recognition. Beyond conventional gas-sensor arrays, a new approach has been reported to leverage the unique gas selectivity of various materials to construct memristor arrays. This

study utilized SnO₂, HfO₂, and Ta₂O₅-based memristors, which exhibit resistance changes in response to gas interactions. These memristors demonstrated varying sensitivities to specific gases and concentrations, enabling the simultaneous detection of mixed gases. A parallel array significantly improved the accuracy of mixed-gas concentration predictions, outperforming single-device systems by over 796% compared to individual Ta₂O₅-based sensors. This advancement underscores the potential of memristor-based sensor technology to enhance environmental monitoring and improve the accuracy and reliability of gas detection in complex gas environments.¹¹⁷

6.2. Protection in dangerous gas environment

The olfactory system plays a crucial role in human awareness, perception, and action in response to diverse external gaseous stimuli. The coordination of olfactory receptors and muscles enables humans to respond to specific gases, which is crucial for protection in dangerous environments, such as in the case of leakage of toxic gases or rooms on fire. However, studies on the functions of the human olfactory system based on memristor devices involving perception, memorization, and self-protection movements are lacking. To emulate a complete olfactory system, an artificial olfactory system should be developed to memorize gas information and control muscles to ensure self-protection in dangerous environments.

Recently, bioinspired olfactory systems that enable the perception and memory of specific gases with the ability to act in the presence of certain gases have been reported. Gas-sensing visualization using a smart robot was developed for real-time gas monitoring by integrating gas sensors and memory devices (Fig. 10a).¹¹⁸ The robot was equipped with an artificial olfactory memory system developed to recognize and memorize volatile organic compound (VOCs) gases at different concentrations. The integration of the sensor and memory unit facilitated the switching of the synaptic memristor in response to the VOCs gas and recorded the target gas information after the gas stimuli disappeared. Additionally, the system was reconfigured with an LED to enhance the gas detection visualization. When concentrations of VOCs were detected below the threshold, the LED remained off. However, if the VOC concentration exceeds the threshold, the LED immediately brightens and remains on. These capabilities of the olfactory system present great potential for future humanoid robots, environmental pollution control, and early warning of chemical and biohazard safety to alert and respond to emergencies in dangerous environments.

In addition to warning about hazardous gases, the flexible artificial olfactory system shown in Fig. 10b can recognize, memorize, and perform self-protection actions for NH₃ and was developed by integrating Sr-ZnO-based gas sensors, HfO_x-based memristors, and electrochemical actuators.¹¹⁹ The gas sensor and synaptic memristor are connected in series, such that changes in NH₃ concentration alter the resistance of the gas sensor, which modifies the voltage intensity applied to the synaptic memristor according to the voltage division rule. Thus, the external chemical signals are conveyed as changes in



1 the electrical signals to the memristor through the resistance
 2 variation of the gas sensor. This process plays a crucial role
 3 translating chemical stimuli into electrical signals. When exposed
 4 specific concentrations of NH_3 , the resistance of the gas sensor
 5 decreased sharply; consequently, a voltage (set voltage) sufficient to
 6 switch the synaptic memristor was applied. When the NH_3
 7 concentration was low, the memristor remained inactive, causing
 8 the actuator to remain unresponsive and the gas to flow normally.
 9 Conversely, as the NH_3 concentration increased, the olfactory
 10 memory device was activated, causing the actuator to bend inward
 11 and close into a conical shape, thereby preventing gas from entering
 12 the nasal cavity. Thus, the activation of the memristor triggers the
 13 movement of the electrochemical actuator to block the gas flow
 14 channel, mimicking the self-protective action of the induced muscle
 15 movement of the hand when it smells NH_3 .

16 This section highlights the effective utilization of memristor-based
 17 olfactory systems in humanoid robotics and environmental
 18 monitoring. However, these systems face inherent limitations in
 19 selectivity and sensitivity to various gases. Moreover, there is a need
 20 to develop systems that can detect external gases in real time,
 21 process the data, and execute appropriate responses. This approach
 22 facilitates rapid and accurate reactions to gas leaks and chemical
 23 hazards, significantly improving the efficiency of environmental
 24 monitoring systems.

25 7. Conclusions and Perspectives

26 Memristive artificial sensory systems, inspired by the energy
 27 efficient architecture of biological systems, have been developed to
 28 overcome the technological limitations of conventional CMOS-based
 29 systems. Memristors can emulate the receptors, neurons, and
 30 synapses—the fundamental components of biological sensory
 31 systems. Building on this foundation, memristors enable higher
 32 order functions such as learning, inference, and hazard detection by
 33 mimicking specific biological sensory systems. Table 1 summarizes
 34 how various memristors emulate biological components and
 35 implement sensory characteristics, demonstrating that memristive
 36 artificial sensory systems can effectively replicate the four major
 37 human senses.

38 In this review, we suggested the emulation of receptor, neuron, and
 39 synapse properties using memristors based on an understanding of
 40 their inherent characteristics. Volatile memristors exhibit switching
 41 behavior, transitioning to an ON state when stimuli exceed a specific
 42 threshold and returning to the Off state when stimuli are removed.
 43 This behavior is suitable for simulating receptors and neurons, as
 44 it closely resembles the "threshold" and "relaxation" responses of
 45 biological receptors. In addition, by adjusting stimulus intensity and
 46 duration, volatile memristors can replicate biological phenomena
 47 such as adaptation and sensitization. Moreover, their behavior
 48 closely resembles "the ion channel dynamics" observed in neurons.
 49 When connected to an external circuit, volatile memristors
 50 effectively model spike generation, including LIF and HH models, as
 51 well as neuron spike shapes. Non-volatile memristors, by contrast,
 52 alter their resistance in response to an applied bias and retain their

resistance even after the bias is removed. This characteristic allows
 them to mimic the information storage function of biological
 synapses, where resistance modulation corresponds to "synaptic
 weight" adjustments in response to neural stimuli.

We then discuss the implementation of the four major senses—
 tactile, visual, auditory, and olfactory—in the memristor-based
 artificial sensory system, as illustrated in Fig. 11. Notably, memristors
 enable comprehensive coverage of previously unachievable
 functionalities that play crucial roles in sensory systems and offer
 efficient energy consumption compared to CMOS-based devices and
 memristors (Table 2). In artificial tactile systems, advancements in
 memristor material and structural design have enabled the effective
 emulation of receptor characteristics such as "sensitivity" and
 "adaptability," which were previously challenging to emulate. For
 example, the system demonstrates a function in which the output
 gradually decreases in response to innocuous stimuli. This
 contradicts the conventional belief that reliable signal conversion
 requires a consistent output for identical inputs. This aligns with the
 operational tendencies of biological sensory systems. In the artificial
 visual system, memristors emulate neuron-spiking models with high
 precision to simulate the functions of biological photoreceptors. By
 reducing the output in response to sudden increases in input signals,
 the system facilitates "light intensity detection" and "self-
 protection." Notably, it efficiently extracts and delivers only essential
 information for actions, such as collision avoidance or blinking, from
 vast visual data inputs. Furthermore, while nociceptors have
 predominantly been implemented for tactile stimuli, the
 development of nociceptive functionality that is responsive to visual
 stimuli is particularly remarkable. In the artificial auditory system,
 the memristors are connected to additional circuits that emulate the
 filtering function of the cochlea. This system is designed to recognize
 only specific sound amplitudes based on memristor resistance,
 enabling "speech recognition" in the biological auditory system. This
 represents a significant advancement in artificial auditory systems. In
 the artificial olfactory system, memristors fabricated from gas-
 sensitive materials integrate sensing and switching characteristics.
 This approach allows the detection of external stimuli without an
 additional circuit. Furthermore, memristor resistance varies
 depending on gas type, allowing for "recognition and memorization"
 of specific gases. These findings break the conventional stereotype
 that receptors are solely responsible for stimulus detection while
 synapses manage information storage. Instead, they demonstrate
 that bioinspired and highly efficient system architectures can
 perform multiple functions within a single device. Besides,
 conventional CMOS-based artificial neural systems struggle to
 implement advanced sensory functions. Even if achievable, such
 implementations typically require significant energy consumption
 and extended processing times. In contrast, memristor-based
 artificial sensory systems can efficiently emulate these advanced
 functions.



1 While memristor-based artificial sensory systems demonstrate
 2 extensive potential, key challenges remain to be addressed.
 3 Although progress has been made in using memristors
 4 independently to detect stimuli and mimic sensory system functions,
 5 system-level integration remains challenging. Most implementations
 6 still rely on additional sensors and circuits primarily used for signal
 7 conversion, such as translating the firing frequency of artificial
 8 neurons into a form that other components can process. However,
 9 improving the energy efficiency of this conversion process has not
 10 been well explored. Although memristors themselves consume nJ
 11 pJ-level low energy, integrating them with CMOS-based systems
 12 often introduces mismatches in electrical parameters, requiring
 13 additional circuitry for voltage conversion, signal processing, and
 14 computation. This increases system complexity and overall energy
 15 consumption, limiting memristors' ability to mimic biological sensory
 16 systems fully. Moreover, if memristors cannot be fabricated using
 17 CMOS-compatible materials and processes, chip-level integration
 18 becomes extremely challenging. Without chip-level integration,
 19 memristors and CMOS-based devices or circuits must be
 20 implemented separately, leading to undesirable consequences such
 21 as signal transmission noise, increased energy consumption, and
 22 larger system area. For instance, Section 4.2 discussed a memristor-
 23 based model mimicking the LGMD neuron, which was integrated into
 24 a car robot to generate avoidance behavior based on optic input
 25 signals. However, implementing this system required power
 26 management chips for voltage conversion and counter circuits for
 27 spike frequency calculation, leading to a complex structure with
 28 additional energy consumption. Unfortunately, current research
 29 primarily focuses on enhancing the performance of individual
 30 memristor devices, with limited studies addressing CMOS
 31 compatibility and efficient architectures for seamless integration
 32 with CMOS-based systems. Therefore, developing a more advanced
 33 memristor-based architecture is essential to enable practical and
 34 energy-efficient system integration. Furthermore, addressing the
 35 following challenges is imperative for the advancement of artificial
 36 sensory systems. First, research on advanced data processing to
 37 perform complex tasks is required. Efficient management of
 38 spatiotemporal data requires multiple memristors working in
 39 conjunction, along with mechanisms to compare and integrate data
 40 from each device. Recent studies have primarily focused on single
 41 memristors, with limited algorithms developed for arrays or circuits.
 42 To mimic biological intelligence, it is essential to establish
 43 interconnections among memristors and integrate their functions.
 44 Additionally, research on integrated system-level memristor-based
 45 receptors, neurons, and synapses is significantly lacking. To construct
 46 artificial sensory systems, memristors emulate and integrate
 47 receptors, neurons, and synapses. However, most studies focus on
 48 them in isolation rather than as part of a cohesive system. Achieving
 49 more efficient conversion and data processing between system
 50 components is essential for accurately replicating biological sensory
 51 functions. For artificial sensory systems to function reliably, research
 52 must focus on compatible signal conversion between the pre- and
 53 post-components. These investigations have the potential to
 54 advance the overall integration of sensory systems by enabling
 55 electrical processing of neural signals for information transmission
 56 and ensuring accurate execution of output signals. In conclusion,
 57 this review provides a framework for implementing memristive artificial

58 sensory systems based on the characteristics of biological
 59 components and switching properties of memristors.
 60

Author Contributions

J. E. Kim and K. Soh contributed equally to this work. J. E. Kim and K. Soh conceived the review and wrote the manuscript. S. I. Hwang and D. Y. Yang reviewed the manuscript. J. H. Yoon supervised the review and finalized the manuscript. All authors have approved the final version of the manuscript.

Conflicts of interest

The authors declare no conflict of interests.

Data availability

No primary research results, software, or codes were involved, and no new data were generated or analyzed as part of this review.

Acknowledgements

This research was supported by the National R&D Program through the National Research Foundation of Korea (NRF) and the Korea Basic Science Institute (National Research Facilities and Equipment Center), and funded by the Ministry of Science and ICT (RS-2024-00406418, NRF-2022R1C1C1004176, and RS-2024-00403917).

Notes and references

1. P. K. Paritala, S. Manchikatla and P. K. D. V. Yarlagadda, *Procedia Engineering*, 2017, **174**, 982-991.
2. U. Rosolia, X. Zhang and F. Borrelli, *Annual Review of Control, Robotics, and Autonomous Systems*, 2018, **1**, 259-286.
3. Y. LeCun, Y. Bengio and G. Hinton, *Nature*, 2015, **521**, 436-444.
4. Z. Wang, S. Joshi, S. Savel'Ev, W. Song, R. Midya, Y. Li, M. Rao, P. Yan, S. Asapu, Y. Zhuo, H. Jiang, P. Lin, C. Li, J. H. Yoon, N. K. Upadhyay, J. Zhang, M. Hu, J. P. Strachan, M. Barnell, Q. Wu, H. Wu, R. S. Williams, Q. Xia and J. J. Yang, *Nature Electronics*, 2018, **1**, 137-145.
5. P. M. Sheridan, F. Cai, C. Du, W. Ma, Z. Zhang and W. D. Lu, *Nat Nanotechnol*, 2017, **12**, 784-789.
6. S. Seo, S. H. Jo, S. Kim, J. Shim, S. Oh, J. H. Kim, K. Heo, J. W. Choi, C. Choi, S. Oh, D. Kuzum, H. P. Wong and J. H. Park, *Nat Commun*, 2018, **9**, 5106.
7. S. Chen, Z. Lou, D. Chen and G. Shen, *Adv Mater*, 2018, **30**.
8. S. Kumar, R. S. Williams, Z. Wang, *Nature* 2020, **585**, 518.
9. J. Wu, Y. Chua, M. Zhang, H. Li and K. C. Tan, *Front Neurosci*, 2018, **12**, 836.
10. H. Kalita, A. Krishnaprasad, N. Choudhary, S. Das, D. Dev, Y. Ding, L. Tetard, H. S. Chung, Y. Jung, T. Roy, *Scientific Reports* 2019, **9**, 1.



- 1 11. P. Stoliar, J. Tranchant, B. Corraze, E. Janod, M. Besland, F. Tesler, M. Rozenberg, L. Cario, *Advanced Functional Materials* 2017, **27**, 62-64.
- 2 12. X. Zhang, J. Lu, Z. Wang, R. Wang, J. Wei, T. Shi, C. Dou, Z. Wu, J. Zhu, D. Shang, G. Xing, M. Chan, Q. Liu, M. Liu, *Science Bulletin* 2021, **66**, 1624. X. Zhang, J. Lu, Z. Wang, R. Wang, J. Wei, T. Shi, C. Dou, Z. Wu, J. Zhu, D. Shang, G. Xing, M. Chan, Q. Liu, M. Liu, *Science Bulletin* 2021, **66**, 1624.
- 3 13. I. Polykretis, G. Tang, P. Balachandar and K. Michmizos, *IEEE Transactions on Medical Robotics and Bionics*, 2022, **4**, 520-529.
- 4 14. W. Shi, J. Cao, Q. Zhang, Y. Li and L. Xu, *IEEE Internet Things Journal*, 2016, **3**, 637-646.
- 5 15. A. Vanarse, A. Osseiran and A. Rassau, *Front Neurosci* 2016, **10**, 115.
- 6 16. I. T. Wang, C. C. Chang, L. W. Chiu, T. Chou, T. H. Hou, *Nanotechnology* 2016, **27**.
- 7 17. M. Prezioso, F. Merrih-Bayat, B. D. Hoskins, G. C. Adams, K. K. Likharev and D. B. Strukov, *Nature*, 2015, **521**, 64-68.
- 8 18. S. Choi, J. Yang and G. Wang, *Advanced Materials*, 2023, **32**, 1-26.
- 9 19. D. S. Jeong, K. M. Kim, S. Kim, B. J. Choi and C. S. Hwang, *Advanced Electronic Materials*, 2016, **2**, 1-27.
- 10 20. H. Li, S. Wang, X. Zhang, W. Wang, R. Yang, Z. Sun, W. Feng, P. Lin, Z. Wang, L. Sun and Y. Yao, *Advanced Intelligent Systems*, 2021, **3**, 2100017-2100017.
- 11 21. J. Park, *Electronics (Switzerland)*, 2020, **9**, 1-16.
- 12 22. R. Yang, H. M. Huang and X. Guo, *Advanced Electronic Materials*, 2019, **5**.
- 13 23. F. Cai, J. M. Correll, S. H. Lee, Y. Lim, V. Bothra, Z. Zhang, M. P. Flynn and W. D. Lu, *Nature Electronics*, 2019, **2**, 290-299.
- 14 24. J. F. Yang, A. T. Liu, T. A. Berrueta, G. Zhang, A. Brooks, V. B. Koman, S. Yang, X. Gong, T. D. Murphy and M. S. Strano, *Advanced Intelligent Systems*, 2022, **4**, 2100205.
- 15 25. S. Wang, S. Gao, C. Tang, E. Occhipinti, C. Li, S. Wang, H. Zhao, G. Hu, A. Nathan, R. Dahiya and L. Occhipinti, *Nature Communications*, 2024, **15**, 4671.
- 16 26. Z. Cao, L. Xiang, B. Sun, K. Gao, J. Yu, G. Zhou, X. Du, W. Yan, F. Lin, Z. Li, R. Wang, Y. Lv, F. Ren, Y. Yao and W. Lu, *Materials Today Bio*, 2024, **26**, 101096.
- 17 27. M. Rao, H. Tang, J. Wu, W. Song, M. Zhang, W. Yin, Z. Zhuo, F. Kiani, B. Chen, X. Jiang, H. Liu, H.-Y. Chen, M. Midya, F. Ye, H. Jiang, Z. Wang, M. Wu, M. Hu, H. Wang, Q. Xia, N. Ge, J. Li and J. J. Yang, *Nature*, 2023, **615**, 820-829.
- 18 28. X. Zhang, Y. Zhuo, Q. Luo, Z. Wu, R. Midya, Z. Wang, W. Song, R. Wang, N. K. Upadhyay, Y. Fang, F. Kiani, M. Yang, Q. Xia, Q. Liu, M. Liu and J. J. Yang, *Nature Communications*, 2020, **11**, 1-9.
- 19 29. F. Li, R. Wang, C. Song, M. Zhao, H. Ren, S. Wang, D. Liang, D. Li, X. Ma, B. Zhu, H. Wang and Y. Hao, *Nano*, 2021, **15**, 16422-16431.
- 20 30. Q. Wu, B. Dang, C. Lu, G. Xu, G. Yang, J. Wang, X. Chu, N. Lu, D. Geng, H. Wang and L. Li, *Nano Lett*, 2020, **20**, 8015-8023.
- 21 31. J. K. Han, D. M. Geum, M. W. Lee, J. M. Yu, S. K. Kim, Kim and Y. K. Choi, *Nano Lett*, 2020, **20**, 8781-8788.
- 22 32. G. Indiveri, B. Linares-Barranco, R. Legenstein, Deligeorgis and T. Prodromakis, *Nanotechnology*, 2013, **24**, 384010.
- 23 33. G. W. Burr, R. M. Shelby, A. Sebastian, S. Kim, S. Kim, S. Sidler, K. Virwani, M. Ishii, P. Narayanan, A. Fumarola, L. L. Sanches, I. Boybat, M. Le Gallo, K. Moon, J. Woo, H. Hwang and Y. Leblebici, *Advances in Physics: X*, 2017, **2**, 89-124.
- 24 34. Q. Wan, M. T. Sharbati, J. R. Erickson, Y. Du and F. Xiong, *Advanced Materials Technologies*, 2019, **4**, 1-34.
- 25 35. B. Joo, J. W. Han and B. S. Kong, *IEEE Transactions on Circuits and Systems I: Regular Papers*, 2022, **69**, 3632-3642.
- 26 36. X. Yan, J. Niu, Z. Fang, J. Xu, C. Chen, Y. Zhang, Y. Sun, L. Tong, J. Sun, S. Yin, Y. Shao, S. Sun, J. Zhao, M. Lanza, T. Ren, J. Chen and P. Zhou, *Materials Today*, 2024, **80**, 365-373.
- 27 37. Y. Pei, L. Yan, Z. Wu, J. Lu, J. Zhao, J. Chen, Q. Liu and X. Yan, *ACS Nano*, 2021, **15**, 17319-17326.
- 28 38. Y. Pei, B. Yang, X. Zhang, H. He, Y. Sun, J. Zhao, P. Chen, Z. Wang, N. Sun, S. Liang, G. Gu, Q. Liu, S. Li and X. Yan, *Nature Communications*, 2025, **16**, 48.
- 29 39. S. Kumar, X. Wang, J. P. Strachan, Y. Yang and W. D. Lu, *Nature Reviews Materials*, 2022, **7**, 575-591.
- 30 40. F. Qin, Y. Zhang, H. W. Song and S. Lee, *Materials Advances*, 2023, **4**, 1850-1875.
- 31 41. Y. Zhang, Z. Wang, J. Zhu, Y. Yang, M. Rao, W. Song, Y. Zhuo, X. Zhang, M. Cui, L. Shen, R. Huang and J. Joshua Yang, *Journal*, 2020, **7**.
- 32 42. S. Kumar, R. S. Williams and Z. Wang, *Nature*, 2020, **585**, 518-523.
- 33 43. J. U. Woo, H. G. Hwang, S. M. Park, T. G. Lee and S. Nahm, *Applied Materials Today*, 2020, **19**, 100582-100582.
- 34 44. S. R. Zhang, L. Zhou, J. Y. Mao, Y. Ren, J. Q. Yang, G. H. Yang, X. Zhu, S. T. Han, V. A. L. Roy and Y. Zhou, *Advanced Materials Technologies*, 2019, **4**.
- 35 45. I. T. Wang, C. C. Chang, L. W. Chiu, T. Chou and T. H. Hou, *Nanotechnology*, 2016, **27**.
- 36 46. X. Yan, L. Zhang, H. Chen, X. Li, J. Wang, Q. Liu, C. Lu, J. Chen, H. Wu and P. Zhou, *Advanced Functional Materials*, 2018, **28**, 1-10.
- 37 47. X. Zhang, W. Wang, Q. Liu, X. Zhao, J. Wei, R. Cao, Z. Yao, X. Zhu, F. Zhang, H. Lv, S. Long and M. Liu, *IEEE Electron Device Letters*, 2018, **39**, 308-311.
- 38 48. H. Kalita, A. Krishnaprasad, N. Choudhary, S. Das, D. Dev, Y. Ding, L. Tetard, H. S. Chung, Y. Jung and T. Roy, *Scientific Reports*, 2019, **9**, 1-8.
- 39 49. P. Stoliar, J. Tranchant, B. Corraze, E. Janod, M. P. Besland, F. Tesler, M. Rozenberg and L. Cario, *Advanced Functional Materials*, 2017, **27**.
- 40 50. X. Zhang, J. Lu, Z. Wang, R. Wang, J. Wei, T. Shi, C. Dou, Z. Wu, J. Zhu, D. Shang, G. Xing, M. Chan, Q. Liu and M. Liu, *Science Bulletin*, 2021, **66**, 1624-1633.
- 41 51. C. Yoon, G. Oh and B. H. Park, *Journal*, 2022, **12**.
- 42 52. C. Wan, P. Cai, M. Wang, Y. Qian, W. Huang and X. Chen, *Advanced Materials*, 2020, **32**, 1902434.
- 43 53. J. Y. Kwon, J. E. Kim, J. S. Kim, S. Y. Chun, K. Soh and J. H. Yoon, *Exploration*, 2024, **4**, 20220162.
- 44 54. A. D. Craig, *Nature reviews neuroscience*, 2002, **3**, 655-666.



- 1 55. S. Cohen and M. E. Greenberg, *Annual review of cell and developmental biology*, 2008, **24**, 183-209. 63
- 2 64
- 3 56. Y. H. Jung, B. Park, J. U. Kim and T. i. Kim, *Advanced Materials*, 2019, **31**, 1803637. 65
- 4 66
- 5 57. J. Sandkuhler, *Physiological reviews*, 2009, **89**, 707-756. 67
- 6 58. R. Wang, J.-Q. Yang, J.-Y. Mao, Z.-P. Wang, S. Wu, 68
- 7 Zhou, T. Chen, Y. Zhou and S.-T. Han, *Advanced Intelligent Systems*, 2020, **2**, 2000055. 70
- 8 71
- 9 59. G. Zhou, Z. Wang, B. Sun, F. Zhou, L. Sun, H. Zhao, X. H. 71
- 10 X. Peng, J. Yan, H. Wang, W. Wang, J. Li, B. Yan, D. Kuan, 72
- 11 Y. Wang, L. Wang and S. Duan, *Advanced Electronic Materials*, 2022, **8**, 2101127. 74
- 12 75
- 13 60. T. Moon, K. Soh, J. S. Kim, J. E. Kim, S. Y. Chun, K. Cho, 75
- 14 Yang and J. H. Yoon, *Materials Horizons*, 2024. 76
- 15 61. A. Vanarse, A. Osseiran and A. Rassau, *Sensors*, 2017, 177
- 16 2591. 78
- 17 62. J. K. Han, S. Y. Yun, S. W. Lee, J. M. Yu and Y. K. Cho, 79
- 18 *Advanced Functional Materials*, 2022, **32**, 2204102. 80
- 19 63. X. Zhang, W. Wang, Q. Liu, X. Zhao, J. Wei, R. Cao, Z. Yao, 81
- 20 X. Zhu, F. Zhang and H. Lv, *IEEE Electron Device Letters*, 82
- 21 2017, **39**, 308-311. 83
- 22 64. G. Wei and I. H. Stevenson, *Neural computation*, 2021, 84
- 23 **33**, 2682-2709. 85
- 24 65. Q. Cheng, S.-H. Song and G. J. Augustine, *Frontiers in synaptic neuroscience*, 2018, **10**, 33. 86
- 25 87
- 26 66. H. R. Monday, T. J. Younts and P. E. Castillo, *Annual review of neuroscience*, 2018, **41**, 299-322. 88
- 27 89
- 28 67. G. Koch, V. Ponzo, F. Di Lorenzo, C. Caltagirone and 90
- 29 Veniero, *Journal of Neuroscience*, 2013, **33**, 9725-9739. 91
- 30 68. T. Guo, K. Pan, Y. Jiao, B. Sun, C. Du, J. P. Mills, Z. Chen, 92
- 31 X. Zhao, L. Wei, Y. N. Zhou and Y. A. Wu, *Nanoscale Horizons*, 2022, **7**, 299-310. 94
- 32 95
- 33 69. S. H. Jo and W. Lu, *Nano Letters*, 2008, **8**, 392-397. 95
- 34 70. S. Chun, J. S. Kim, Y. Yoo, Y. Choi, S. J. Jung, D. Jang, 96
- 35 Lee, K. I. Song, K. S. Nam, I. Youn, D. Son, C. Pang, 97
- 36 Jeong, H. Jung, Y. J. Kim, B. D. Choi, J. Kim, S. P. Kim, 98
- 37 Park and S. Park, *Nature Electronics*, 2021, **4**, 429-438. 99
- 38 71. D. Wang, L. Wang, W. Ran, S. Zhao, R. Yin, Y. Yan, 100
- 39 Jiang, Z. Lou and G. Shen, *Nano Energy*, 2020, 101
- 40 105109-105109. 102
- 41 72. K. He, Y. Liu, M. Wang, G. Chen, Y. Jiang, J. Yu, C. Wu, 103
- 42 D. Qi, M. Xiao, W. R. Leow, H. Yang, M. Antonietti and 104
- 43 Chen, *Advanced Materials*, 2020, **32**. 105
- 44 73. Y. Lee, J. Park, A. Choe, S. Cho, J. Kim and H. 106
- 45 *Advanced Functional Materials*, 2019, **30**. 107
- 46 74. D. Dev, M. S. Shawkat, A. Krishnaprasad, Y. Jung and 108
- 47 Roy, *IEEE Electron Device Letters*, 2020, **41**, 1440-1443. 109
- 48 75. M. D. Schaffler, L. J. Middleton and I. Abdus-Saboor, 110
- 49 *Psychiatry Rep*, 2019, **21**, 134. 111
- 50 76. J. H. Yoon, Z. Wang, K. M. Kim, H. Wu, V. Ravichandran, 112
- 51 Q. Xia, C. S. Hwang and J. J. Yang, *Nature Communications*, 2018, **9**, 417. 114
- 52 77. Y. Kim, Y. J. Kwon, D. E. Kwon, K. J. Yoon, J. H. Yoon, 115
- 53 Yoo, H. J. Kim, T. H. Park, J.-W. Han, K. M. Kim and 116
- 54 Hwang, *Advanced Materials*, 2018, **30**, 1704320. 117
- 55 78. R. A. John, N. Tiwari, M. I. B. Patdillah, M. R. Kulkarni, 118
- 56 Tiwari, J. Basu, S. K. Bose, Ankit, C. J. Yu, A. Nirmal, 119
- 57 Vishwanath, C. Bartolozzi, A. Basu and N. Mathe, 120
- 58 *Nature Communications*, 2020, **11**, 1-12. 121
- 59 79. S. Maksimovic, M. Nakatani, Y. Baba, A. M. Nelson, 122
- 60 Marshall, S. A. Wellnitz, P. Firozi, S.-H. Woo, S. Ran, 123
- 61 and A. Patapoutian, *Nature*, 2014, **509**, 617-621. 124
- 62
80. E. L. Graczyk, B. P. Delhay, M. A. Schiefer, S. J. Bensmaia and D. J. Tyler, *Journal of neural engineering*, 2018, **15**, 046002. DOI: 10.1039/D5MH00039F
81. Y. G. Song, J. M. Suh, J. Y. Park, J. E. Kim, S. Y. Chun, J. U. Kwon, H. Lee, H. W. Jang, S. Kim, C. Y. Kang and J. H. Yoon, *Advanced Science*, 2022, **9**, 1-10.
82. C. Wan, G. Chen, Y. Fu, M. Wang, N. Matsuhisa, S. Pan, L. Pan, H. Yang, Q. Wan, L. Zhu and X. Chen, *Advanced Materials*, 2018, **30**.
83. C. Wang, L. Dong, D. Peng and C. Pan, *Advanced Intelligent Systems*, 2019, **1**.
84. Y. Lee and J. H. Ahn, *ACS Nano*, 2020, **14**, 1220-1226.
85. M. Wang, J. Tu, Z. Huang, T. Wang, Z. Liu, F. Zhang, W. Li, K. He, L. Pan, X. Zhang, X. Feng, Q. Liu, M. Liu and X. Chen, *Advanced Materials*, 2022, **34**, 1-8.
86. X. Pan, J. Wang, Z. Deng, Y. Shuai, W. Luo, W. Luo, Q. Xie, Y. Xiao, S. Tang, S. Jiang, C. Wu, F. Zhu, J. Zhang and W. Zhang, *Advanced Intelligent Systems*, 2022, **4**, 2200031-2200031.
87. Q. Duan, T. Zhang, C. Liu, R. Yuan, G. Li, P. Jun Tiw, K. Yang, C. Ge, Y. Yang and R. Huang, *Advanced Intelligent Systems*, 2022, **4**, 2200039.
88. H. Kafaligonul, *The Journal of Neurobehavioral Sciences*, 2014, **1**.
89. D. L. Yamins, H. Hong, C. F. Cadieu, E. A. Solomon, D. Seibert and J. J. DiCarlo, *Proc Natl Acad Sci U S A*, 2014, **111**, 8619-8624.
90. Y. Mohsenzadeh, C. Mullin, B. Lahner and A. Oliva, *Sci Rep*, 2020, **10**, 4638.
91. M. H. Herzog and A. M. Clarke, *Front Comput Neurosci*, 2014, **8**, 135.
92. Yang, G. R., & Wang, X. J. Artificial neural networks for neuroscientists: a primer. *Neuron*, 2020, **107(6)**, 1048-1070.
93. B. Dang, K. Liu, X. Wu, Z. Yang, L. Xu, Y. Yang and R. Huang, *Advanced Materials*, 2022, DOI: 10.1002/adma.202204844.
94. X. Shan, C. Zhao, X. Wang, Z. Wang, S. Fu, Y. Lin, T. Zeng, X. Zhao, H. Xu, X. Zhang and Y. Liu, *Advanced Science*, 2022, **9**.
95. Y. Xu, S. Gao, Z. Li, R. Yang and X. Miao, *Advanced Intelligent Systems*, 2022, **4**, 2200210-2200210.
96. Y. Pei, Z. Li, B. Li, Y. Zhao, H. He, L. Yan, X. Li, J. Wang, Z. Zhao, Y. Sun, Z. Zhou, J. Zhao, R. Guo, J. Chen and X. Yan, *Advanced Functional Materials*, 2022, **32**.
97. Y. Wang, Y. Gong, S. Huang, X. Xing, Z. Lv, J. Wang, J. Q. Yang, G. Zhang, Y. Zhou and S. T. Han, *Nature Communications*, 2021, **12**.
98. J. Li, Y. Zhou, Y. Li, C. Yan, X.-G. Zhao, W. Xin, X. Xie, W. Liu, H. Xu and Y. Liu, *ACS Photonics*, 2024, **11**, 4578-4587.
99. L. Ng, M. W. Kelley and D. Forrest, *Nat Rev Endocrinol*, 2013, **9**, 296-307.
100. J. H. Lee, M. Y. Lee, Y. Lim, J. Knowles and H. W. Kim, *J Tissue Eng*, 2018, **9**, 2041731418808455.
101. M. Cortada, S. Levano and D. Bodmer, *Int J Mol Sci*, 2021, **22**.
102. L. Sun, Y. Zhang, G. Hwang, J. Jiang, D. Kim, Y. A. Eshete, R. Zhao and H. Yang, *Nano Letters*, 2018, **18**, 3229-3234.
103. B. Gao, Y. Zhou, Q. Zhang, S. Zhang, P. Yao, Y. Xi, Q. Liu, M. Zhao, W. Zhang, Z. Liu, X. Li, J. Tang, H. Qian and H. Wu, *Nature Communications*, 2022, **13**.



- 1 104. F. Moro, E. Hardy, B. Fain, T. Dalgaty, P. Cl emen on, 57 127. X. Wang, C. Chen, L. Zhu, K. Shi, B. Peng, Y. Zhu, H. Mao, 58
2 De Pr a, E. Esmanhotto, N. Castellani, F. Blard, F. Gardien, 58
3 T. Mesquida, F. Rummens, D. Esseni, J. Casas, G. Indiveri, 59
4 M. Payvand and E. Vianello, *Nature Communications*, 2022, **13**, 61
5 2022, **13**. 61
6 105. L. Cheng, L. Gao, X. Zhang, Z. Wu, J. Zhu, Z. Yu, Y. Yang, 62 129. X. Shan, C. Zhao, X. Wang, Z. Wang, S. Fu, Y. Lin, T. Zeng,
7 Y. Ding, C. Li, F. Zhu, G. Wu, K. Zhou, M. Wang, T. Shi and 63
8 Q. Liu, *Frontiers in Neuroscience*, 2022, **16**. 64
9 106. F. Moro, E. Hardy, B. Fain, T. Dalgaty, P. Cl emen on, 65 130. J. Yu, F. Zeng, Q. Wan, Z. Lu and F. Pan, *InfoMat*, 2023,
10 De Pr a, E. Esmanhotto, N. Castellani, F. Blard, F. Gardien, 66 5, e12458.
11 T. Mesquida, F. Rummens, D. Esseni, J. Casas, G. Indiveri, 67 131. B. Gao, Y. Zhou, Q. Zhang, S. Zhang, P. Yao, Y. Xi, Q. Liu,
12 M. Payvand and E. Vianello, *Nature Communications*, 2022, **13**, 3506. 69
13 107. S. Seo, B. S. Kang, J. J. Lee, H. J. Ryu, S. Kim, H. Kim, 70 132. F. Moro, E. Hardy, B. Fain, T. Dalgaty, P. Cl emen on, A.
14 Oh, J. Shim, K. Heo, S. Oh and J. H. Park, *Nature 71
15 Communications*, 2020, **11**. 72
16 108. A. Rinaldi, *EMBO Rep*, 2007, **8**, 629-633. 73
17 109. K. E. Whitlock and M. F. Palominos, *Front Neuroanat*, 74
18 2022, **16**, 831602. 75 133. C. Sbandati, S. Stathopoulos, P. Foster, N. D. Peer, C.
19 110. C. Huart, P. Rombaux and T. Hummel, *Molecules*, 2012, **18**, 11586-11600. 77
20 111. G. M. Shepherd, *Nature*, 2006, **444**, 316-321. 78 134. R. Chaurasiya, K.-T. Chen, L.-C. Shih, Y.-C. Huang and J.-
21 112. A. L. Saive, J. P. Royet and J. Plailly, *Front Behav Neurosci*, 79
22 2014, **8**, 240. 80
23 113. Q. Lu, F. Sun, Y. Dai, Y. Wang, L. Liu, Z. Wang, S. Wang 81 135. L. Wang, W. Li, L. Wan and D. Wen, *ACS Sensors*, 2023,
24 and T. Zhang, *Nano Research*, 2021, **15**, 423-428. 82 8, 4810-4817.
25 114. T. Wang, X.-X. Wang, J. Wen, Z.-Y. Shao, H.-M. Huang 83 136. T. Wang, H.-M. Huang, X.-X. Wang and X. Guo, *InfoMat*,
26 and X. Guo, *Advanced Intelligent Systems*, 2022, **4**. 84 2021, **3**, 804-813
27 115. J.-K. Han, M. Kang, J. Jeong, I. Cho, J.-M. Yu, K.-J. Yoon, 85 137. P. Qiu, Y. Qin and Q. Xia, *Sensors and Actuators B: Chemical*, 2022, **373**, 132730.
28 Park and Y.-K. Choi, *Advanced Science*, 2022, **8**, 86
29 2106017. 87
30 116. S. Y. Chun, Y. G. Song, J. E. Kim, J. U. Kwon, K. Soh, J. 88 138. Y. Yoon, Y. Kim, W. S. Hwang and M. Shin, *Advanced
31 Kwon, C.-Y. Kang and J. H. Yoon, Advanced Materials*, 2023, **35**, 2302219. 89
32 117. D. Lee, M. J. Yun, K. H. Kim, S. Kim and H.-D. Kim, *ACS 90 139. Y. Qin, M. Wu, N. Yu, Z. Chen, J. Yuan and J. Wang, ACS
33 Sensors*, 2021, **6**, 4217-4224. 92 Applied Electronic Materials, 2024, **6**, 4939-4947.
34 118. C. Ban, X. Min, J. Xu, F. Xiu, Y. Nie, Y. Hu, H. Zhang, 93 140. J.-K. Han, M. Seo, W.-K. Kim, M.-S. Kim, S.-Y. Kim, M.-S.
35 Eginligil, J. Liu, W. Zhang and W. Huang, *Advanced 94
36 Materials Technologies*, 2021, **6**. 95
37 119. Z. Gao, S. Chen, R. Li, Z. Lou, W. Han, K. Jiang, F. Qu and 96 141. J.-K. Han, J. Oh, G.-J. Yun, D. Yoo, M.-S. Kim, J.-M. Yu, S.-
38 G. Shen, *Nano Energy*, 2021, **86**. 97 Y. Choi and Y.-K. Choi, *Science Advances*, 2021, **7**,
39 120. D. Chen, X. Zhi, Y. Xia, S. Li, B. Xi, C. Zhao and X. Wang, 98 eabg8836.
40 *Small*, 2023, **19**, 2301196. 99 142. L. Wang, L. Zhang, S. Hua, Q. Fu and X. Guo, *Science
41 China Materials*, 2025, 1-8.
42 100
43 100
44 J. Huang, J. Feng, Z. Chen, Z. Dai, S. Yang, Z. Chen, H. Zhang, 101 143. S. Seo, B. Kim, D. Kim, S. Park, T. R. Kim, J. Park, H. Jeong,
45 Zhou, Z. Zeng, X. Li and X. Gui, *Nano Energy*, 2024, **126**, 109684. 103
46 123. L. Xiaoqi, J. Jianbo, L. Guangyu, Z. Bao and Z. Enmiao, 104 144. J. Park, Y. Jang, J. Lee, S. An, J. Mok and S. Y. Lee,
47 *Journal of Materials Science: Materials in Electronics*, 2024, **35**, 1608 106
48 2024, **35**, 1608 106
49 124. Z. Lv, S. Zhu, Y. Wang, Y. Ren, M. Luo, H. Wang, G. Zhang, 107 145. X. Yan, Q. Zhao, A. P. Chen, J. Zhao, Z. Zhou, J. Wang, H.
50 Y. Zhai, S. Zhao, Y. Zhou, M. Jiang, Y.-B. Leng and S. Han, 108
51 *Advanced Materials*, 2024, **36**, 2405145. 109
52 125. J. Shi, Y. Lin, Z. Wang, X. Shan, Y. Tao, X. Zhao, H. Xu and 110
53 Y. Liu, *Advanced Materials*, 2024, **36**, 2314156. 111
54 126. Y. Gong, X. Xing, X. Wang, R. Duan, S.-T. Han and B. K. 112
55 Tay, *Advanced Functional Materials*, 2024, **34**, 2406547
56 112



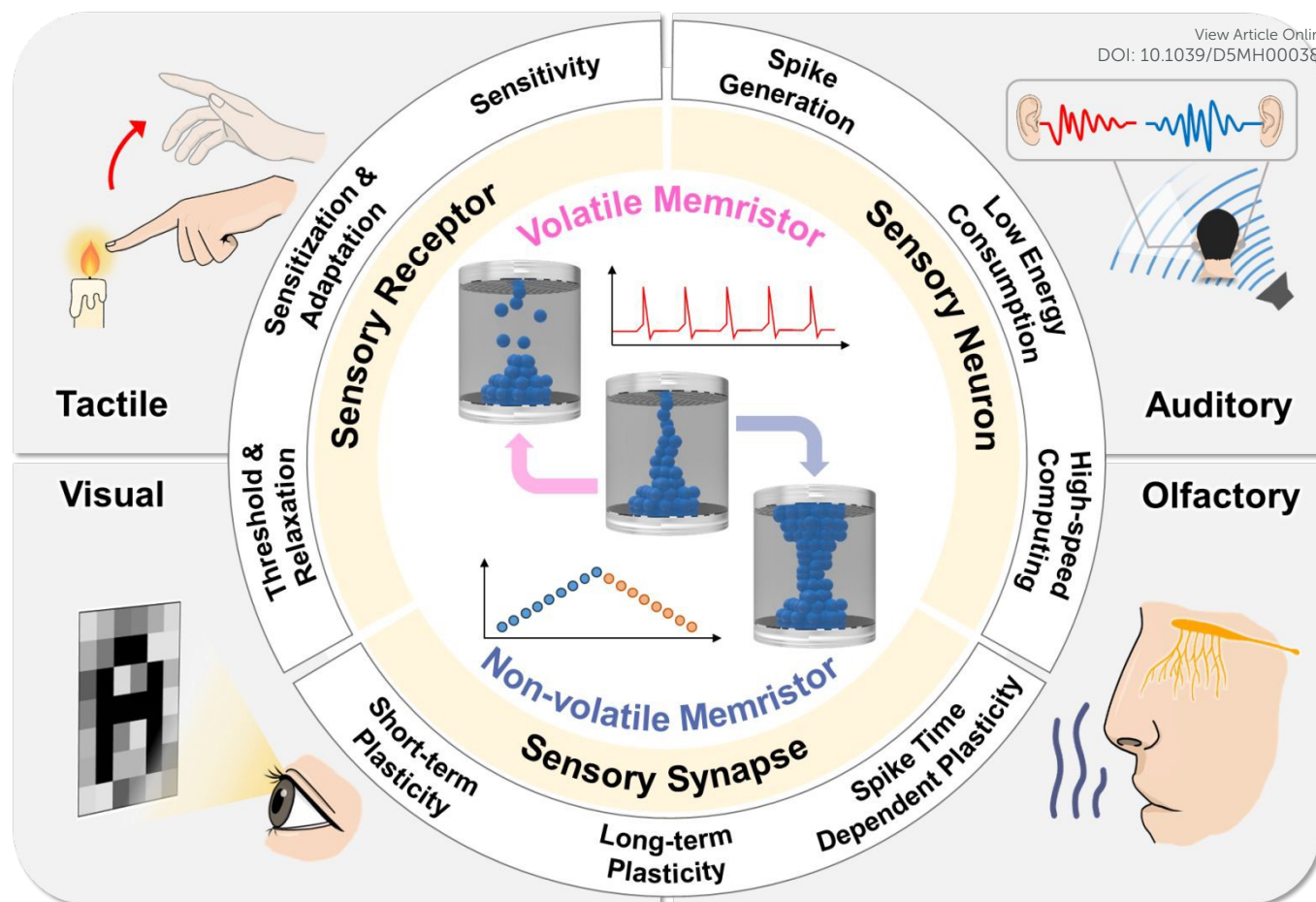


Fig. 1 Schematic of the artificial sensory system and functions, featuring integrated and collaborative networks of memristive receptors, neurons, and synapses.



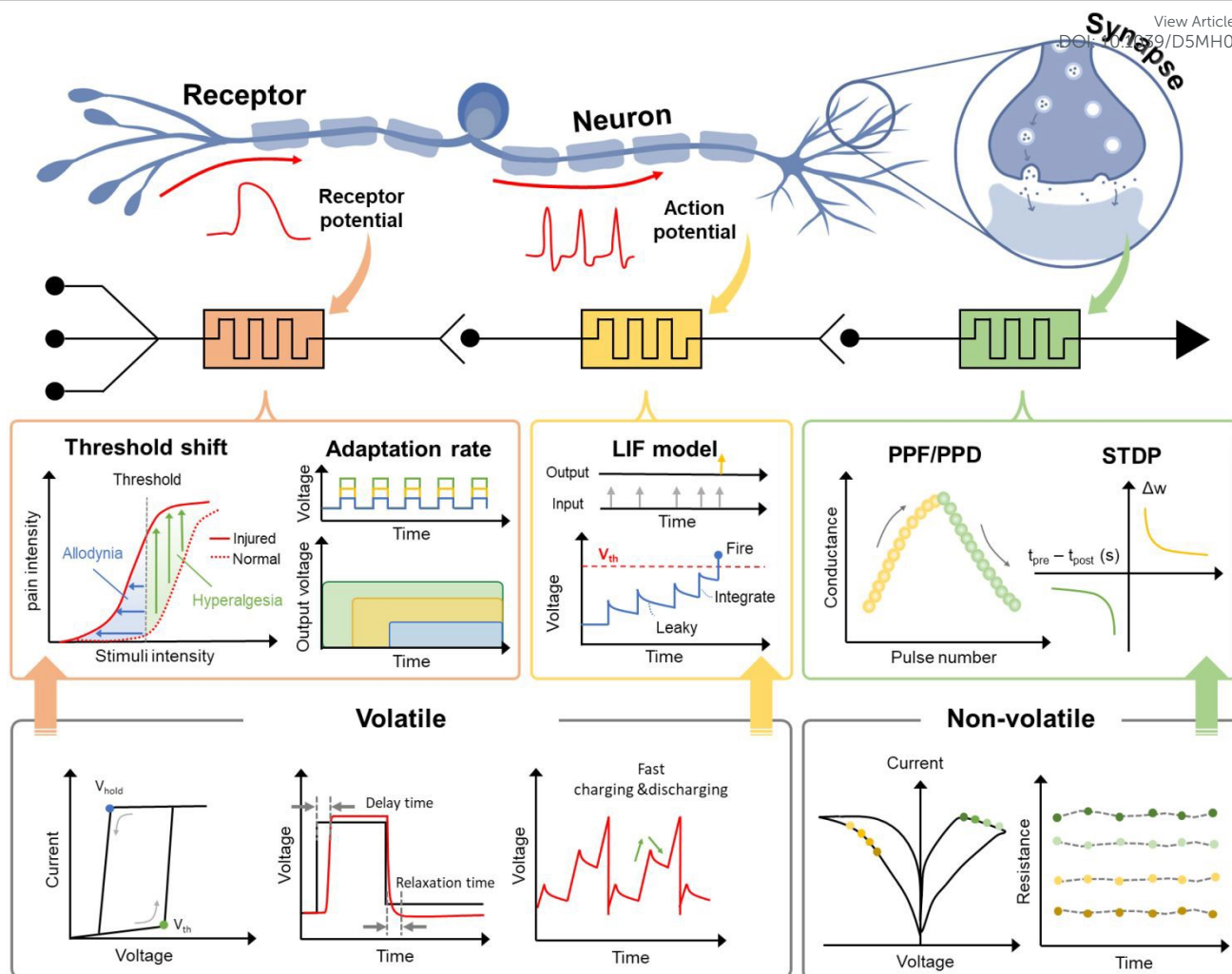


Fig. 2 Features and performances required to implement artificial sensory receptors, neurons, and synapses. Function characteristics of volatile and non-volatile memristors to mimic sensory elements.



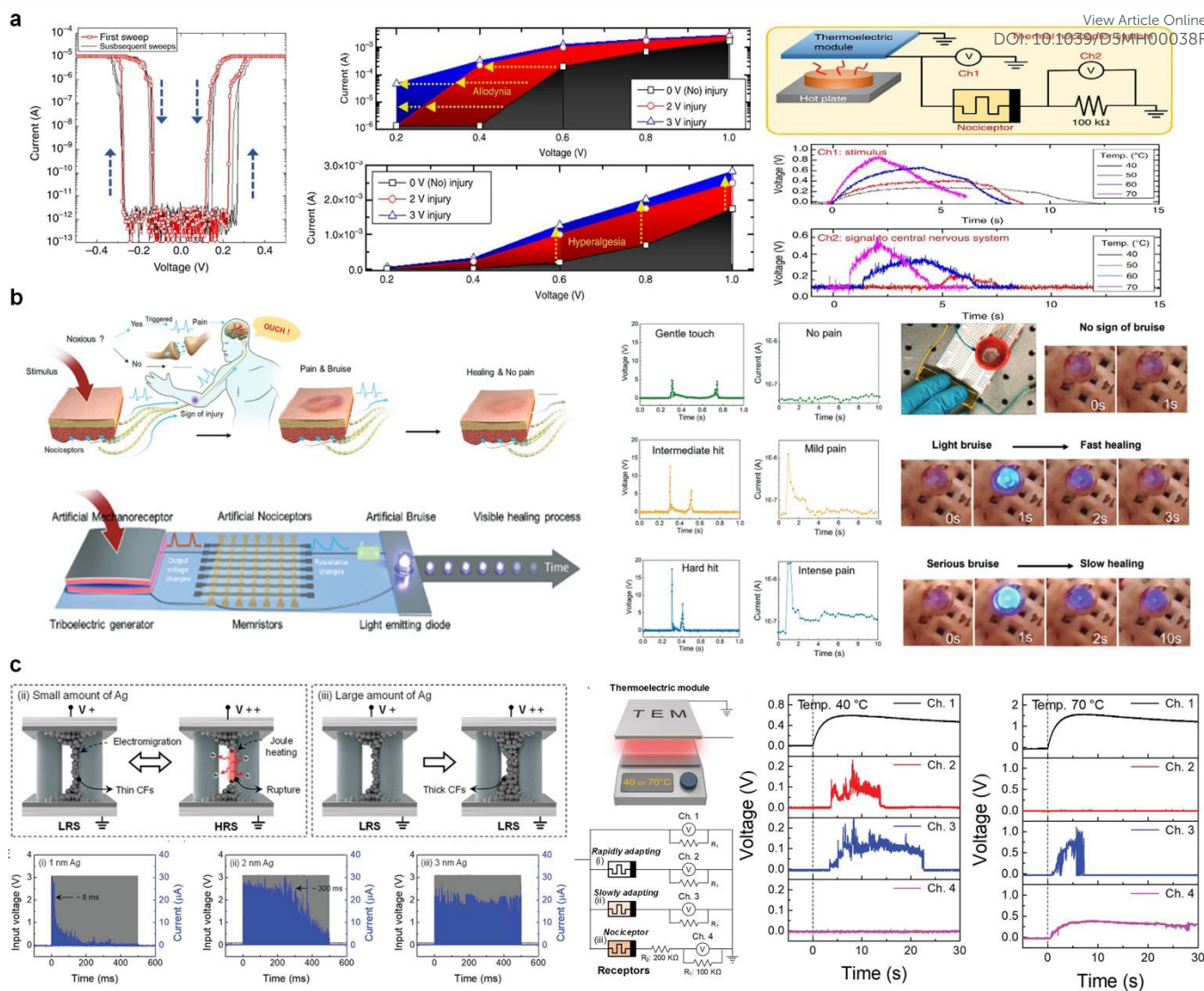


Fig. 3 (a) Threshold switching behavior, allodynia, and hyperalgesia. Schematic of an artificial thermal nociceptor circuit comprising a thermoelectric module and a volatile memristor. Generated voltage by thermoelectric module and threshold switching behavior. Reproduced with permission from ref. 76. Copyright 2018 Springer Nature (b) Bio-inspired artificial injury response system including a sense of pain, sign of injury, and healing. Lighting of light-emitting diodes (LEDs) according to intensity of stimulation. Reproduced with permission from ref. 78. Copyright 2022 John Wiley and Sons (c) Pulse response of memristors to multiple 100 μ s pulse widths with an amplitude of 3 V. Adaptation rates of 1, 2, and 3 nm Ag memristors are classified as rapidly, slowly, and no-adapting, respectively. Circuit schematic of an artificial sensory nervous system. Generated voltage from the thermoelectric module and volatile memristors was monitored by oscilloscope channels at hot plate temperatures of 40 and 70 °C. Reproduced with permission from ref. 81. Copyright 2021 John Wiley and Sons



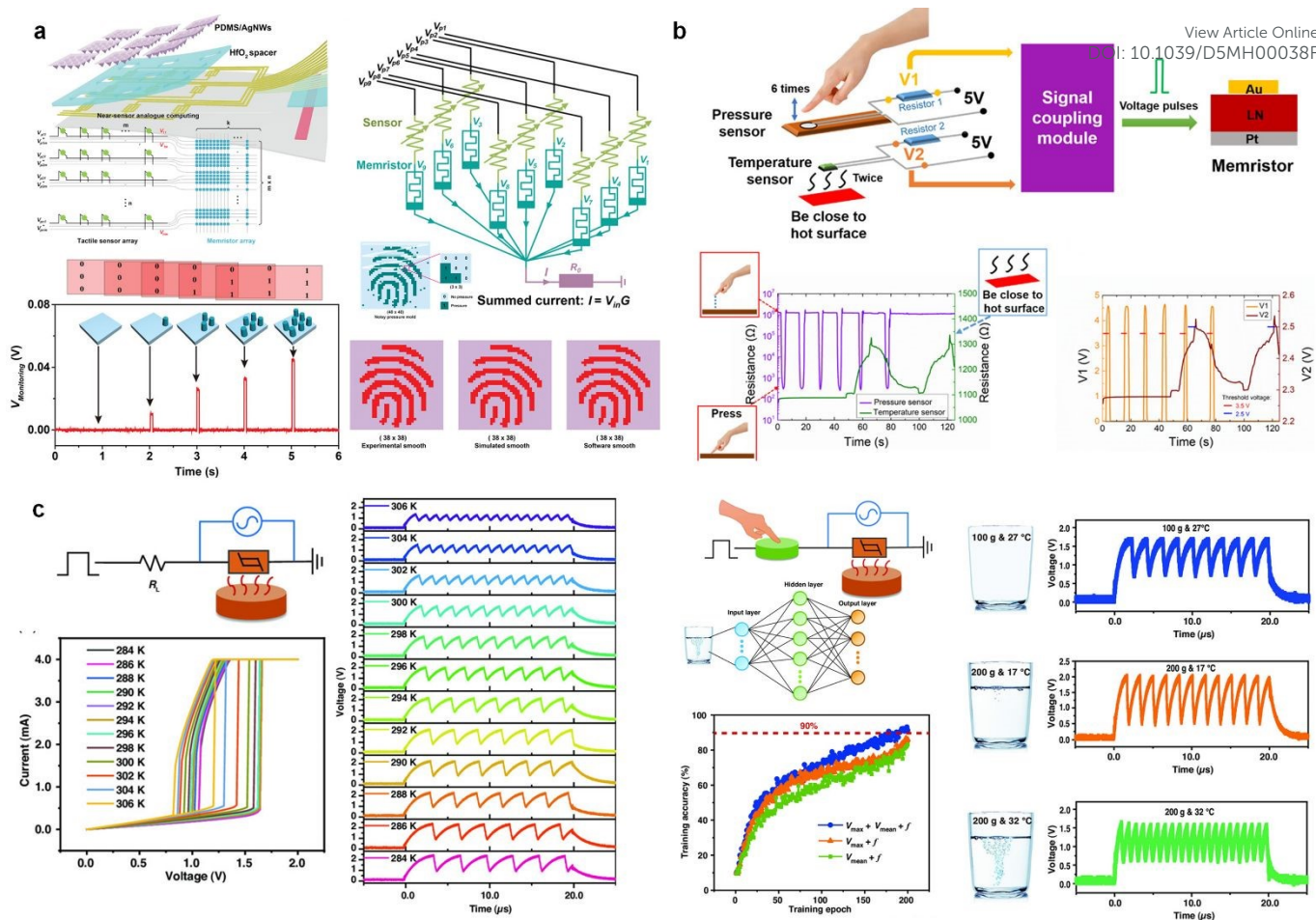


Fig. 4 (a) Near-sensor analog computing using artificial tactile system. Resistance changes in synapse memristor using a continuous pulse train. Near-sensor analog computing for real-time edge detection of the captured pressure pattern. Reproduced with permission from ref. 85. Copyright 2022 John Wiley and Sons (b) Multimodal sensory system with multi-sensors accepting pressure and temperature stimuli. Resistance modulation of the pressure and temperature sensors as a response to pressure and hot stimuli. Reproduced with permission from ref. 86. Copyright 2022 John Wiley and Sons (c) Characterization of artificial temperature perception VO₂-based neuron memristor. Haptic-temperature fusion is based on a VO₂ volatile memristor and MLP by simulation. Reproduced with permission from ref. 87. Copyright 2022 John Wiley and Sons



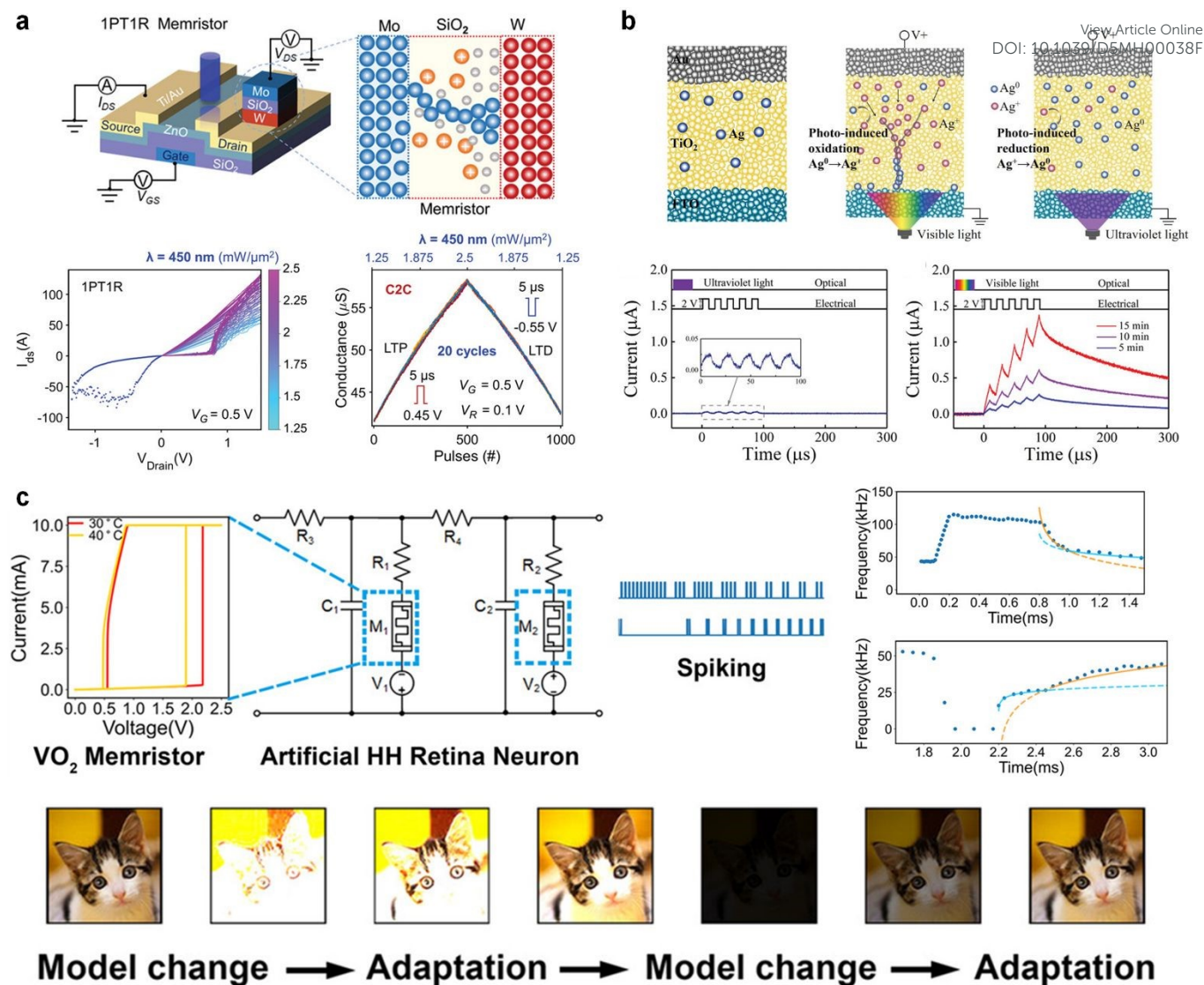


Fig. 5 (a) Schematic illustration of the integrated 1PT1R structure device and light-tunable conductance update performance of the device. Reproduced with permission from ref. 93. Copyright 2023 John Wiley and Sons (b) Schematic illustration of light-induced synaptic modification mechanism based on photo-induced redox reaction and current response after UV/Vis light irradiation. Reproduced with permission from ref. 94 Copyright 2021 John Wiley and Sons (c) Bio-inspired HH neuron for artificial retinal system with firing frequency modulated in a manner similar to photopic/scotopic adaptation of a biological photoreceptor. Reproduced with permission from ref. 95. Copyright 2022 John Wiley and Sons



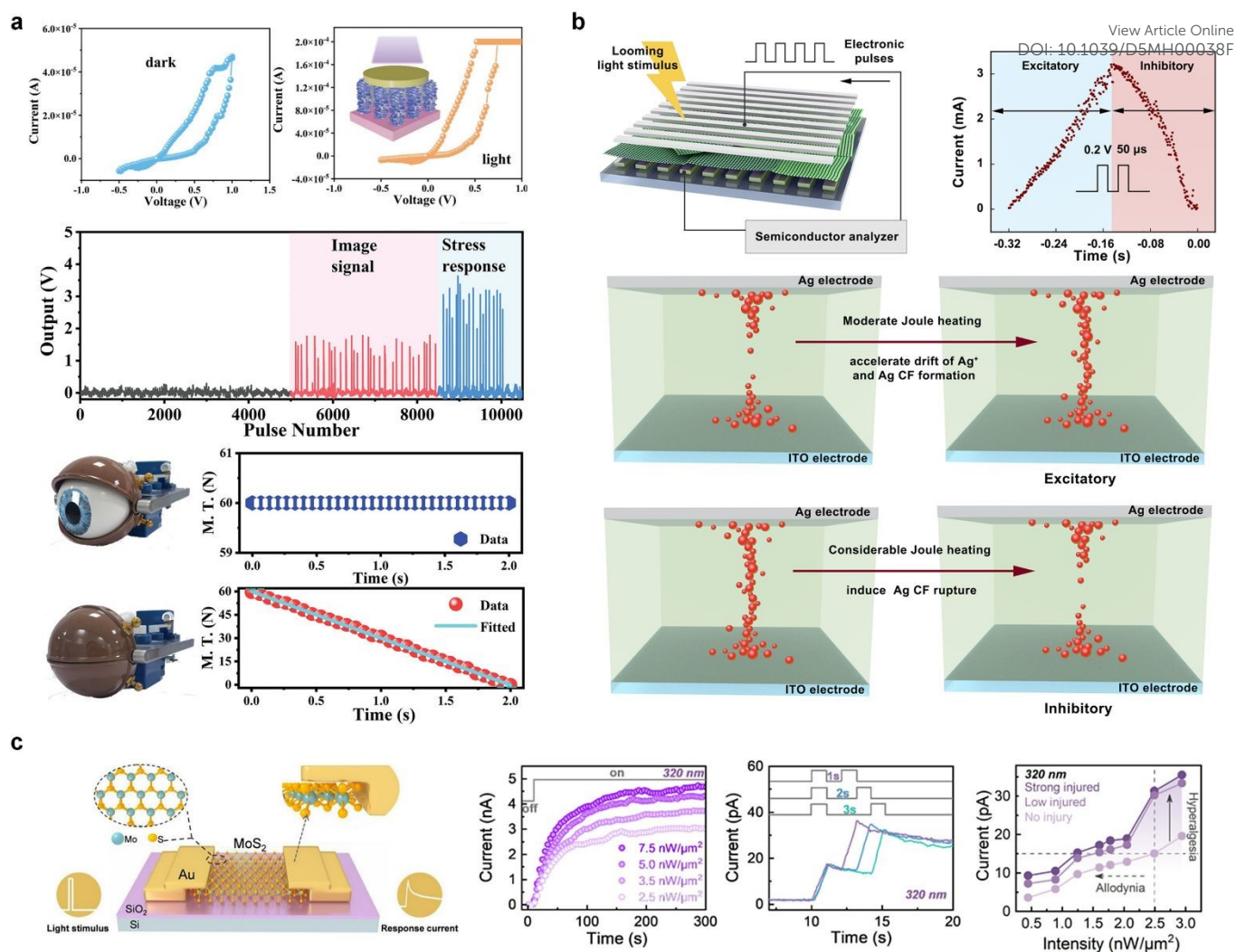


Fig. 6 (a) Multifunctional artificial visual perception nervous system using optoelectronic memristor based on an Sb_2Se_3 nanorod array. Increasing ON/OFF resistance ratio under light irradiation increases the firing frequency, activating an eyelid-shaped actuator. Reproduced with permission from ref. 96. Copyright 2022 John Wiley and Sons (b) Schematics of the artificial LGMD neuron device and current response under looming light stimulus. The formation of the Ag conductive filament is initially facilitated by the increasing light stimulus but ruptures due to Joule heating beyond a certain light intensity, providing information before the collision point. Reproduced with permission from ref. 97. Copyright 2021 Springer Nature (c) Schematic of the monolayer MoS_2 device and current response under varying light intensity, pulse interval, and degree of injury. Reproduced with permission from ref. 98. Copyright 2024 American Chemical Society

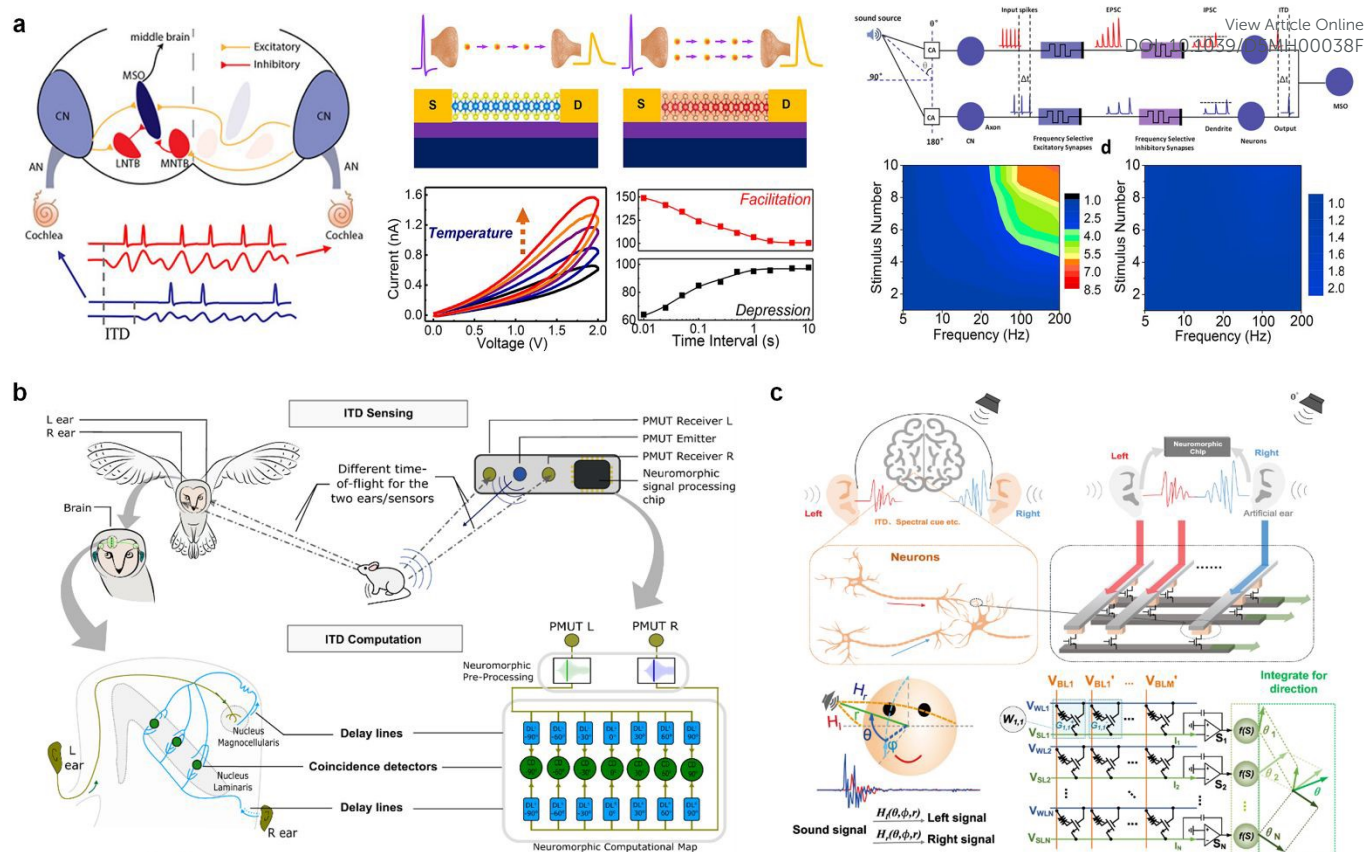


Fig. 7 (a) Schematic of the human auditory perception system and monolayer MoS₂-based device with Joule heating-driven conductance facilitation. ITD-based sound localization can be achieved by suppressing interference and encoding only ITD information through artificial synaptic computation comprising the MoS₂ device. Reproduced with permission from ref. 102. Copyright 2021 American Chemical Society (b) Object localization system in barn owls and proposed bio-inspired technology. Response varies across population, impacting both input gain and time constant. Owing to neuron-to-neuron variability, two output neurons of direction-sensitive coincidence detector respond differently to input stimuli. Thus, sound source can be identified. Reproduced with permission from ref. 103. Copyright 2022 Springer Nature (c) Conceptual diagram of memristor-based neuromorphic sound localization system. Multiple binaural features applied for neural processing to detect sound sources, including binaural time difference, spectral shape, etc. Reproduced with permission from ref. 104. Copyright 2022 Springer Nature



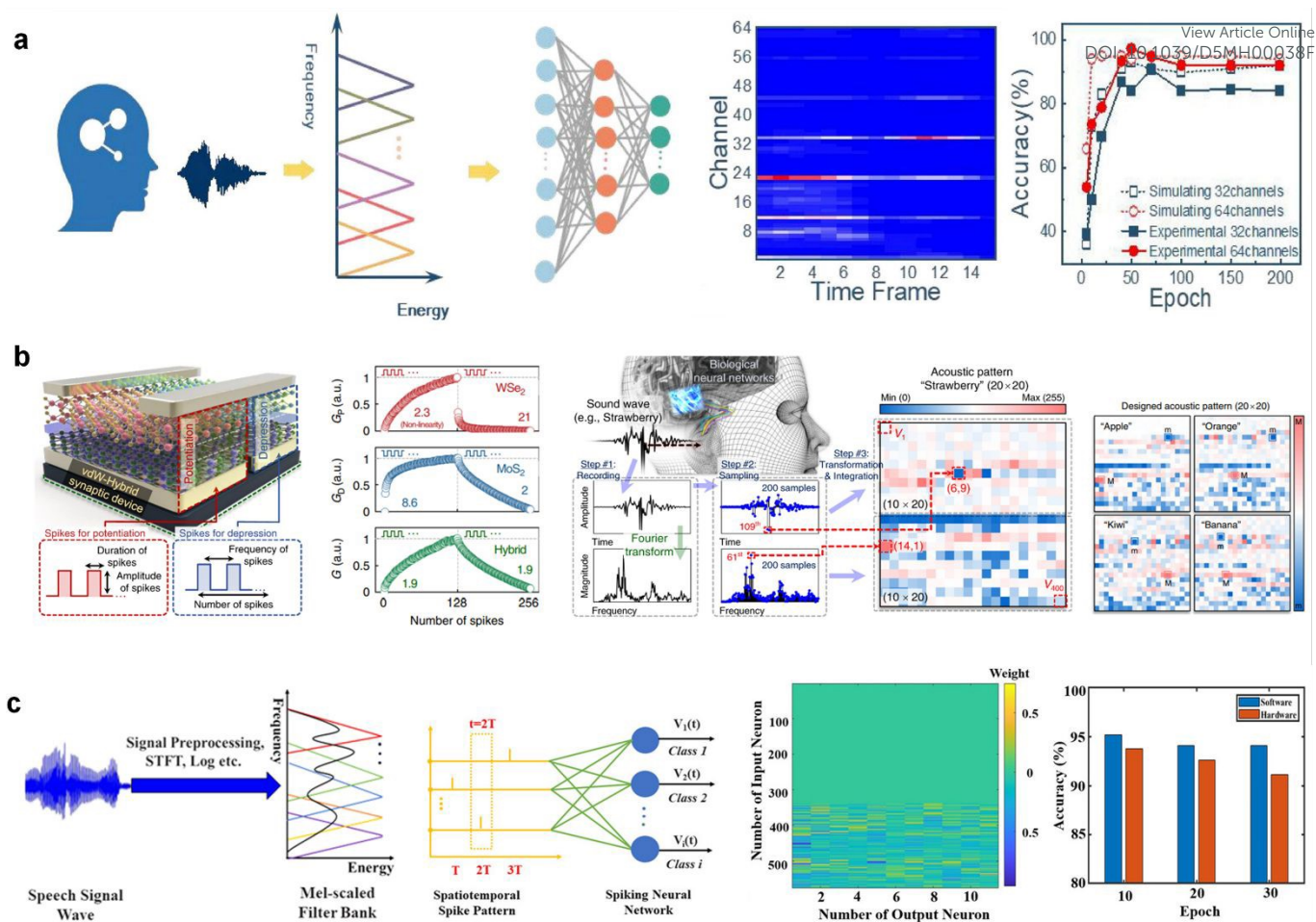


Fig. 8 (a) Schematic of artificial cochlea speech recognition system used to demonstrate frequency-selection function of five channels in the cochlea. Channels have central frequencies determined by the resistance of a memristor. It achieved a recognition accuracy of 92% using 64 channels. Reproduced with permission from ref. 104. Copyright 2022 Frontiers Media S.A. (b) Design procedure of acoustic pattern (from recording, through transforming, to integrating). The van der Waals hybrid synapse was utilized to perform acoustic pattern recognition, a common task in speech and sound processing. Reproduced with permission from ref. 105. Copyright 2020 Springer Nature (c) Schematic of feature extraction from speech signals. Extracting features from speech signals enables successful training of SNN in both software- and memristor-based implementations, resulting in accurate classification inference. Reproduced with permission from ref. 107. Copyright 2021 John Wiley and Sons



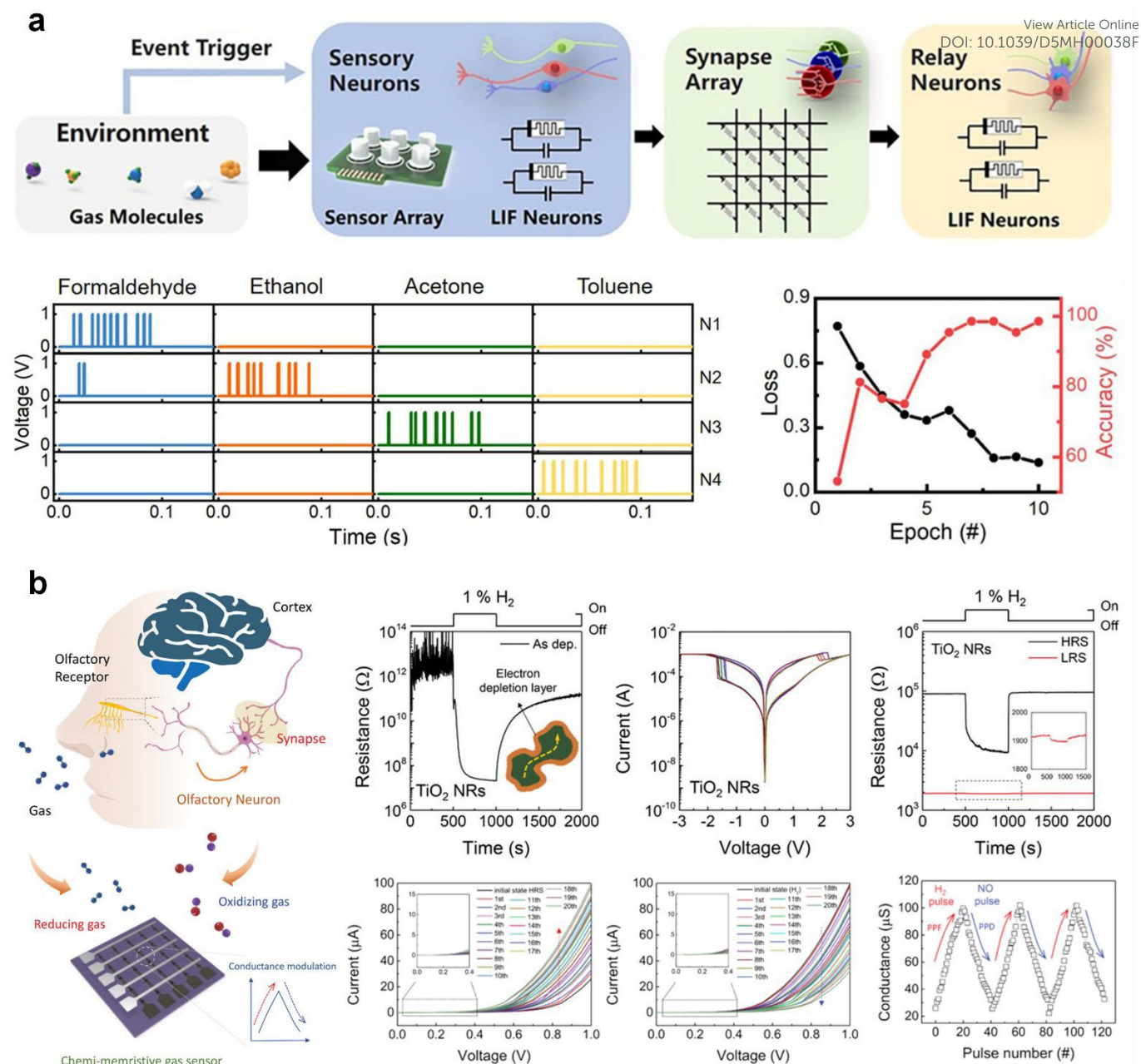


Fig. 9 (a) Bio-inspired neuromorphic olfactory system based on the memristive neural network comprising a gas sensor, sensory neurons, synapse arrays, and relay neurons. Sampling voltages in the LIF neuron. Larger input signals (red lines) results in shorter capacitor charging times (green lines), quicker device switching (blue lines), and higher output frequencies (orange lines). Training loss and testing accuracy of detection gas. Reproduced with permission from ref. 103. Copyright 2022 John Wiley and Sons (b) Schematic of biological olfactory cognitive process mimicking using chemi-memristive sensor. Response curves upon exposure to 1% H₂ and *I-V* curves of TiO₂ NRs. Conductance modulations based on type of target gas (reducing or oxidizing). Reproduced with permission from ref. 104. Copyright 2023 John Wiley and Sons



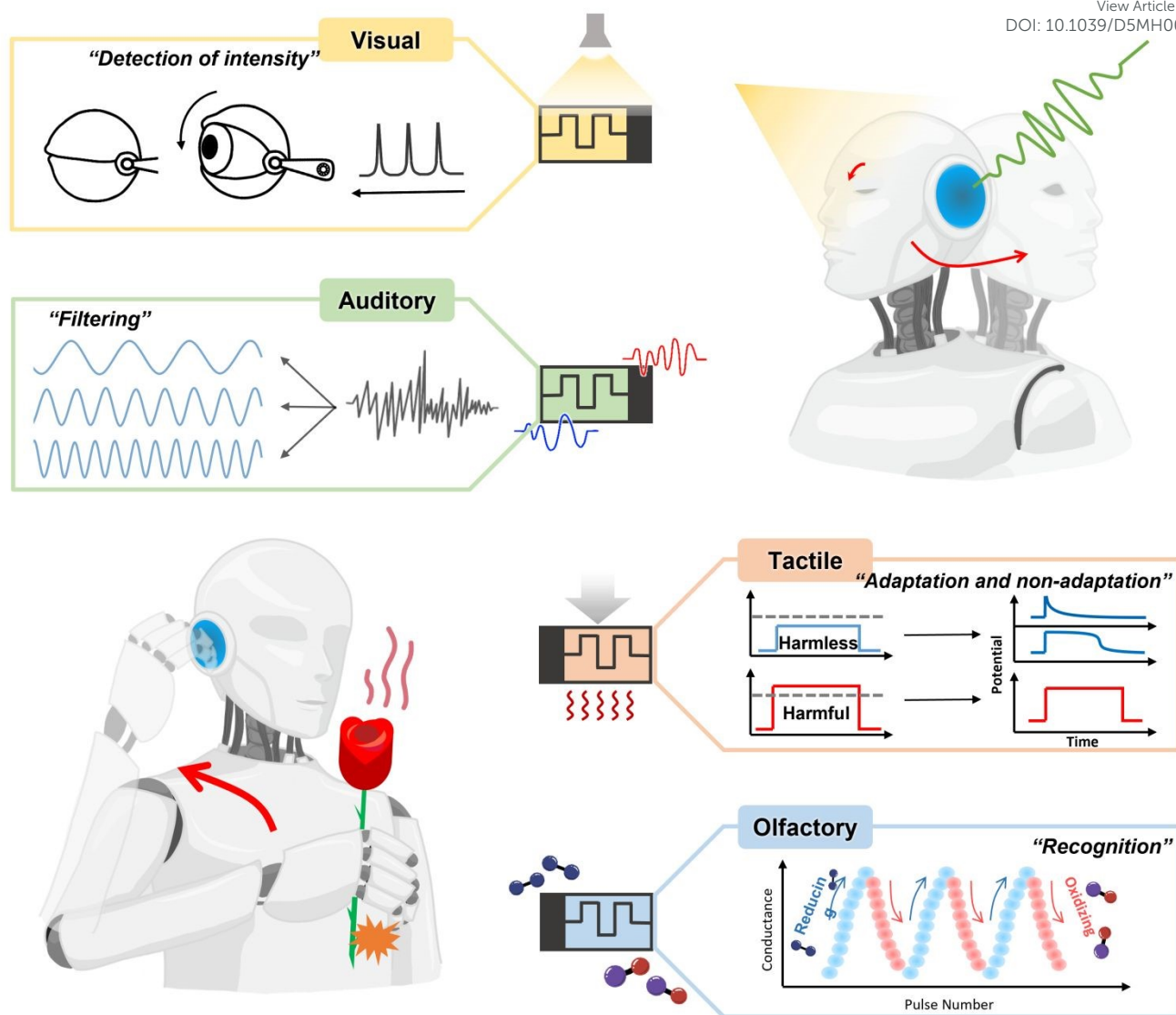


Fig. 11 Schematic of biological and artificial sensory systems with a memristor.



Table 1. A summary of memristive artificial sensory systems.

View Article Online

DOI: 10.1039/D5MH00038F

Sense	Memristor	Materials & Structure	Biological Counterpart	Specific feature	Ref
Tactile	Non-volatile	Ag/CsPbBr ₃ /PVA/FTO	Synapse	Mechanoreceptor (Pressure)	120
	Non-volatile	Al/CS:MWCNTs/ITO	Synapse	Mechanoreceptor (Pressure)	121
	Non-volatile	Ag/TiO _x /Ti ₃ C ₂ Tx/Au	Neuron	Mechanoreceptor (Pressure)	122
	Volatile	Al/ZnO/FTO	Synapse	Nociceptor	123
	Volatile	Ag/c-YY NW/Ag	Neuron	Mechanoreceptor (Humidity)	124
Visual	Volatile	Al/Ag NW-embedded SA/SA/ITO	Synapse/Neuron	Scotopic /photopic adaptation	125
	Volatile	Cr/Au/WS ₂ /Cr/Au	Synapse	Color recognition	126
	Volatile	ITO/Ta ₂ O ₅ /Ag/IGZO/ITO	Neuron	Color recognition	127
	Volatile/non-volatile	FTO/NiO/Organic Interlayer/PMMA/Ag	Synapse	Color recognition	128
	Volatile/non-volatile	Pd/TiO _x /ZnO/TiN	Synapse	Object tracking	129
Auditory	Volatile	Pd/Nb/NbO _x /Nb/Pd	Synapse	Sound Localization	130
	Non-volatile	TiN/TaO _x /HfO _x /TiN	Synapse	Sound Localization	131
	Non-volatile	TiN/HfO _x /Ti/TiN	Synapse	Object localization	132
	Non-volatile	Pt/TiO _x /AlO _x /Pt	Synapse	Audio-Reward association	133
Olfactory	Non-volatile	Ta/m-ZrO ₂ /Pt	Synapse	Odor recognition	134
	Non-volatile	Al/pectin:Ag NPs/ITO	Synapse	Odor recognition	135
	Volatile/non-volatile	W/WO ₃ /PEDOT:PSS/Pt, Pd/W/WO ₃ /Pd	Synapse/Neuron	Gas-Classification	136
	Non-volatile	-/TiO ₂ Nanowire/ Ti	Sensor	Odor recognition	137



Table 2. Comparison of switching characteristics with CMOS-based devices.

View Article Online

DOI: 10.1039/D5MH00038F

		Structure	Operating voltage	Switching Speed	ION	Ref
Receptor	CMOS	Sn-doped polycrystalline β -Ga ₂ O ₃ FET	10 V (VD)	0.5 s	-	138
	Memristor	Ag/SnSe/Au	Set : 0.474	55 ns	10 μ A	139
Pt/Ag/SiO ₂ NRs/Ag/Pt		Set : - 0.72 V + 0.78 V	20 μ s	1 μ A	81	
Neuron	CMOS	Si-based MOSFET	V _G : -1 V V _D : > 3.5 V	0.1 s	\approx 150 μ A	140
		Si/SiO ₂ /Si ₃ N ₄ /SiO ₂ /Si-based MOSFET	V _G : 12 V V _D : > 3 V	0.02 s	\approx 150 μ A	141
	Memristor	Pt/Ag/TaO _x /Pt	Set : 0.29 V	80 μ s	0.1 μ A	114
		Ag/MoS ₂ nanosheet/ Ag/MoO _x /Ag	Set : 0.3 V	16 ns	100 μ A	31
		Pt/Ag/ZnO/Pt	Set : 0.17 V	\approx 50 ns	10 μ A	142
Synapse	CMOS	Si/WO _x /SiO ₂ -based FET	Write: 1.8 V (V _G) Erase : -2.5 (V _G)	0.3 ms	-	143
		IGZO channel-based FET	Write: 20 V (V _G) Erase : -20 V (V _G)	100 ms (Write) 10 ms (erase)	\approx 10 μ A	144
	Memristor	Pd/WS ₂ /Pt	Set : 0.6 V Reset : -0.2 V	14 ns	1 μ A	145
		Al/PVP-CdSe QD/Al	Set : 0.61 V Reset : -0.5 V	41 ns	5.2 μ A	146
		ITO/CdS QDs-PVP/Al	Set : 1.08 V Reset : -0.72 V	42 ns	4.44 μ A	147

